EVALUATION OF MASONRY WALL PERFORMANCE

UNDER CYCLIC LOADING

By

TIMOTHY PHILLIPS VAUGHAN

A thesis submitted in partial fulfillment of
the requirements for the degree of

MASTER OF SCIENCE IN CIVIL ENGINEERING

WASHINGTON STATE UNIVERSITY
Department of Civil and Environmental Engineering

MAY 2010

To the Faculty of Washington State University:

The members of the Committee appointed to examine the thesis of
TIMOTHY PHILLIPS VAUGHAN find it satisfactory and recommend that it be accepted.

_____

David I. McLean, Ph. D., Chair

_____

David G. Pollock, Ph.D.

_____

Mohamed ElGawady, Ph.D.

ACKNOWLEDGMENTS

I would like to express my deepest gratitude to Dr. David McLean for serving as chair of my committee and for all the support he has provided throughout this project and during my graduate school experience. I would also like to thank Dr. David Pollock for serving on my committee and for the additional advice and guidance provided as an advisor during my first year of graduate school. A thank you is extended to Dr. Mohamed ElGawady for serving on my committee as well.

I also would not have been able to complete this thesis without the support of family and friends. Thank you Magy, Mom, Mike, and Julia for your invaluable encouragement, friendship, and advice the last two years. I would not be who I am today without you.

EVALUATION OF MASONRY WALL PERFORMANCE

UNDER CYCLIC LOADING

Abstract

By Timothy Phillips Vaughan, MS.
Washington State University
May 2010

Chair: David I. McLean

This research evaluated the structural performance of reinforced masonry shear walls conforming to requirements given in the 2008 MSJC *Building Code Requirements for Masonry Structures* under cyclic lateral loading. Seismic design provisions in the 2008 MSJC provide prescriptive requirements for three different wall types corresponding to different levels of expected performance and minimum levels of ductility during a seismic event. Along with load capacity, displacement ductility and drift capacities are important parameters in the seismic design of structures, and there has been recent interest from researchers and designers about the values that can be achieved with the prescriptive provisions of each MSJC wall type.

Ductility and drift values were obtained from a wide range of tests of masonry walls under cyclic loading representative of seismic loading. The test data consisted of results obtained for both fully grouted concrete and clay masonry walls. Each wall was classified to the applicable MSJC wall type and the dominant failure mode (flexure or shear). Statistical analyses were performed to evaluate the performance of each wall type failing in flexure or shear. Theoretical predictions of performance were compared to experimental results for walls failing in flexure. Parametric studies were also performed on both data sets to evaluate the effects of various test parameters on ductility and drift.

The prescriptive requirements in the MSJC for different types of shear walls resulted in levels of ductility and drift performance that aligned with the general intent of the Code. However, significant scatter in the results make it clear that achieving a target level of ductility or performance through the use of the prescriptive provisions alone is unreliable. Further research on walls failing strictly in flexure is recommended to more accurately identify MSJC wall type performance levels. The theoretical predictions of performance for walls failing in flexure were very conservative. Additional research to establish more realistic ultimate strain values for masonry is recommended.

TABLE OF CONTENTS

Page

LIST OF TABLES

LIST OF FIGURES

CHAPTER 1

INTRODUCTION

1.1 Background

Masonry construction is common throughout the world and has been used for millennia due to its ease of construction, low costs, and durability. Early forms of masonry were unreinforced and possessed significant compressive strength and low tensile strength. However, large self-weights of walls and floors were generally sufficient to offset tensile stresses caused by small lateral loads and thus provide for satisfactory performance of masonry structures. During significant earthquakes in the 19th and 20th centuries, however, substantial lateral loads were induced and the vulnerability of sizeable unreinforced masonry construction was revealed (Shedid, 2006). Many masonry structures collapsed or suffered considerable damage, calling into question the safety of unreinforced masonry for a number of applications. Consequently, the development of masonry as a modern construction material was slowed as the use of steel and reinforced concrete became more common.

In regions of low seismic activity, masonry still remained a popular and economical option as a building material, particularly for low-rise construction. Regions of high seismic activity demanded more ductile and earthquake resistant structures, and as a result reinforced masonry was developed. In general, the seismic design of all masonry structures is highly conservative due to the historically poor performance of unreinforced masonry in past earthquakes. However, properly detailed and well constructed reinforced masonry has consistently shown to perform well and provide adequate safety during seismic events.

Shear walls act as the primary components of the lateral load resisting system in masonry construction. They serve to transfer lateral loads from a horizontal diaphragm, such as a roof, to a diaphragm or wall below, or to the foundation. Gravity loads are also carried through the shear walls to the foundation, making shear walls axial load-carrying members as well. Reinforced masonry shear walls naturally exhibit large lateral stiffness and substantial lateral load resistance, which serve to provide adequate performance in seismic events (Shedid, 2006). As a result, they have been used extensively as the chief lateral load resistance system in low- and medium-rise buildings.

The behavior and response of masonry shear walls under simulated seismic loading has been studied since the 1970's. These studies have shown that it is impractical to design shear walls to remain purely elastic in regions of moderate to high seismic activity. Shear walls must be able to undergo inelastic deformations without losing the ability to carry axial loads. Ductility is a parameter commonly used in the evaluation and design of structures as it characterizes the effectiveness of the structure in the inelastic range of deformation.

Seismic design of structures has seen a shift over the last 20 years from a force-based approach to displacement or "performance" based design. Traditional seismic design was based on forces because design for other actions, such as dead or live loadings, was historically based on forces. Force-based seismic design suffers from many fundamental problems. Estimates of initial stiffness are relied upon to distribute forces between structural elements, but the actual stiffness cannot be known until the design is complete. The allocation of forces between elements based on initial stiffness is in itself incorrect because it assumes that the different elements can be forced to yield simultaneously. Force-based design also does not provide a "uniform risk" of damage for structures at a specified level of intensity. The deficiencies of

force-based design and the recognition of the importance of deformation rather than strength in evaluating seismic performance have led to increased use and interest in performance-based design (Priestley, 2007).

Performance or displacement-based design is built upon recognition of the fact that well-designed structures possess ductility and can withstand inelastic deformations imposed by earthquakes without loss of strength. The existence of ductility allows for structures to be designed for less than calculated elastic force levels (Priestley, 2007). Controlled damage in carefully detailed plastic hinges is accepted in order to create more economical designs. Energy dissipation that is associated with ductility is far more important than strength during a seismic event. Peak displacements are critical in determining the performance of the structure and level of damage that can be expected. Therefore it is appropriate to design structures based upon a prescribed displacement or performance level.

The research reported in this thesis is an evaluation of the performance of masonry walls complying with current seismic design provisions in the Masonry Standards Joint Committee (MSJC) *Building Code Requirements and Specifications for Masonry Structures* (MSJC, 2008). The MSJC has different wall types designed for different assumed levels of performance in a seismic event. Minimum levels of ductility are intended to be provided for each wall type through prescriptive provisions. Previous studies by NEHRP (2000), Voon and Ingham (2007), and Davis (2008) assessed shear provisions in various codes through the collection and analysis of experimental studies of masonry shear walls. This research utilizes applicable data from these studies and expands the data to include a number of other experimental studies. The goal of this research is to provide a better understanding of the expected load and displacement performance

of masonry walls to support the development of performance-based design procedures for masonry structures.

1.2. Scope and Objectives

The primary objective of this research is to evaluate the performance of masonry walls complying with current MSJC provisions for seismic design. Collection of data from six previous studies and subsequent statistical analysis of the data yielded displacement ductility and drift values for each MSJC wall type. Wall performance was considered with respect to two different failure modes; flexure and shear. For walls failing in flexure, theoretical values of displacement and displacement ductility were compared to data obtained from experimental testing. Further evaluation of each data set (flexure and shear) evaluated the effects of wall parameters on masonry shear wall behavior. The parameters examined include wall aspect ratio, amount of shear reinforcement, level of axial compressive stress, and amount of vertical reinforcement.

1.3 Thesis Organization

This thesis is composed of five chapters. Chapter 2 contains a review of masonry shear wall failure modes, experimental studies of masonry shear walls, displacement ductility, and MSJC provisions for seismic design of shear walls. Chapter 3 provides a summary of the procedures used in interpreting displacement ductility, drift, MSJC wall types, and other parameters. Chapter 4 provides an evaluation of the performance of masonry shear walls based on calculations made using the interpretations from Chapter 3. Chapter 5 presents conclusions reached in this study along with recommendations for future research on the seismic performance of masonry shear walls.

CHAPTER 2

LITERATURE REVIEW

2.1 Introduction

Numerous experimental and theoretical studies on the seismic behavior of masonry shear walls have been performed since the 1970's. Knowledge of the behavior of shear walls has increased significantly due to these studies. This chapter provides a review of the seismic behavior of reinforced masonry shear walls through examination of shear wall failure modes, experimental studies on the in-plane performance of shear walls, and displacement ductility. The current seismic design provisions given in the 2008 MSJC *Building Code Requirements for Masonry Structures* (MSJC, 2008) are also reviewed.

2.2 Shear Wall Failure Modes

The increased use of reinforced masonry shear wall systems has spurred numerous experimental investigations into the performance and failure modes of such systems. Much of the research has focused on the in-plane behavior of masonry shear walls under cyclic lateral loading (representative of loads induced in a seismic event) and differing combinations of axial load and reinforcement. Several different response mechanisms have been identified under this type of in-plane loading, including flexural, shear, rocking, and sliding failure mechanisms (see Figure 2.1). However, if adequate anchorage is provided, shear and flexure failure mechanisms become dominant and are much more likely to control wall behavior.

Flexural failure is generally preferred, particularly in seismic design, as it is has been shown to correspond with ductile behavior. It is characterized by the tensile yielding of vertical

reinforcement, the formation of one or more plastic hinge zones, and crushing of masonry at critical wall sections (Paulay and Priestley, 1992; Shing et al., 1991; Shedid, 2008). Crushing of the extreme compressive masonry is commonly known as toe crushing and is generally initiated by crushing and vertical splitting of the masonry. Block shell spalling follows the initial splitting and ultimately the grout core is crushed (Eikanas, 2003). Research has indicated that flexural theory and the assumption that plane sections remain plane is a satisfactory representation of walls dominated by flexural behavior (Shing et al., 1990). The increased ductility of the flexural failure mechanism coincides with greater energy dissipation (due to yielding of reinforcement) and superior overall seismic performance. Brittle failures can occur, however, if large amounts of flexural reinforcement are used. In this case, the flexural reinforcement does not yield significantly prior to the extreme masonry compression fiber reaching its critical strain (Eikanas, 2003). As a result, it is important to limit the amount of flexural reinforcement to ensure proper ductility in masonry walls controlled by flexural behavior.

The shear failure mechanism is characterized by diagonal tensile cracking or shear slip along bed joints. Diagonal tensile cracking is seen when the principal diagonal stress exceeds the masonry tensile strength (Voon, 2007). The diagonal cracking strength is mainly dependent on the level of axial stress, the strength of the masonry, and the aspect ratio of the wall. Smaller aspect ratios contribute to greater shear deformations. Before diagonal cracking begins, horizontal and vertical reinforcement in the wall is essentially not engaged and carries little to no load. Shear strength after cracking, however, is dependent upon aggregate interlock forces and the amount of vertical and horizontal reinforcement (Shing et al., 1991). Transverse reinforcement must be properly anchored in order to ensure it contributes sufficiently to the overall shear strength of the wall. Proper anchorage is achieved by providing the transverse

reinforcement with 180° hooks around the extreme vertical reinforcement (Sveinsson et al., 1985). Shear walls dominated by the shear mechanism tend to exhibit brittle behavior and quicker strength degradation after the maximum strength has been reached (Paulay and Priestley, 1992). This type of failure is undesirable in seismic events, as failure or collapse of structures without adequate warning becomes much more likely. The ductility of a wall controlled by a shear failure can be enhanced if sufficient amounts of transverse reinforcement are used and the reinforcement is appropriately anchored (Shing et al., 1991).

Failures due to sliding are characterized by a sliding plane along either a continuous horizontal flexural crack or between two diagonal cracks. Walls under cyclic loading with large amounts of horizontal reinforcement and small amounts of vertical reinforcement are susceptible to a sliding failure (Eikanas, 2003). A lack of friction between the wall base and foundation also contributes to sliding. Under in-plane loading, the slip plane is typically found at the base of the wall due to the non-continuous construction between the footing and the wall base. Sliding is generally initiated by flexural reinforcement yielding along the wall base joint. Large displacements initiate dowel action from the flexural reinforcement and a significant clamping force is developed. Sliding resistance is enhanced as the clamping force increases friction and aggregate interlock forces become effective. Adequate amounts of uniformly distributed flexural reinforcement provide dowel action and a clamping force and can effectively eliminate sliding behavior (Priestley, 1986).

The controlling failure mechanism has been shown through studies to be dependent upon several properties of the wall and the loading conditions. The wall height-to-length ratio (wall aspect ratio), quantity and distribution of horizontal and vertical reinforcement, and magnitude of axial load all factor into the type of failure mechanism that will dominate. In low-aspect ratio

(also known as squat) walls, shear failure is much more likely to govern behavior. The flexural mechanism is more likely to control failure in high aspect ratio walls (Shedid, 2006).

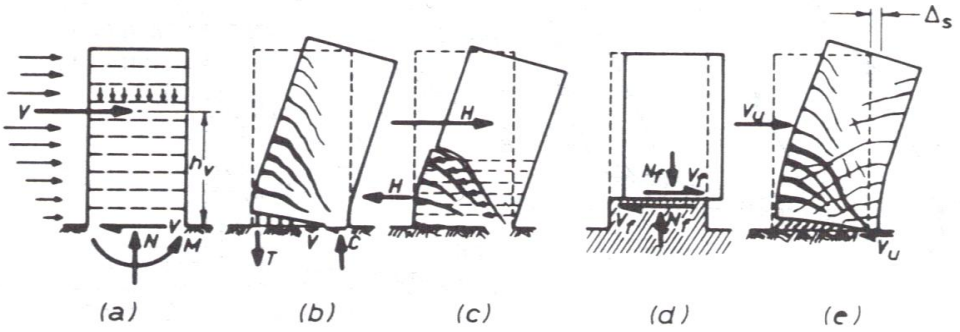

Figure 2.1 Typical cantilever shear wall failure modes. (b) Rocking failure (c) Shear failure (d) Sliding failure (e) Flexural failure (Paulay and Priestley, 1992)

2.3 Cyclic In-plane Masonry Shear Wall Studies

The seismic behavior of reinforced masonry shear walls has been examined through numerous experimental studies since the 1970's. These studies generally consist of cyclic, in-plane, displacement-controlled loading of shear walls with varying dimensions and various levels of axial load and reinforcement. The following section discusses several of these experimental studies and their results.

2.3.1 Shing et al.

Shing et al. (1991) conducted experimental and analytical investigations of the inelastic behavior of concrete and clay masonry shear walls. Sixteen concrete masonry specimens and six clay masonry specimens were subjected to horizontal and axial loading in order to determine the effects of a range of load conditions and design parameters. The amount of vertical and horizontal reinforcement and the level of axial stress served as the variables while the size of each specimen was held constant at 72 in. high by 72 in. wide. Each concrete masonry wall

consisted of a single wythe of either 6 x 8 x 16 in. hollow concrete blocks or 6 x 4 x 16 in. hollow clay bricks. All reinforcement was uniformly distributed at 16 in., with one exception where the spacing of the horizontal reinforcement was reduced to 8 in. All walls were fully grouted and all horizontal reinforcement had 180° hooks around the extreme vertical steel. The cantilever walls were subjected to a constant axial load and cyclic in-plane loading. The testing apparatus and setup is shown in Figure 2.2.

In addition to experimental analysis, the researchers also performed moment-curvature analyses in order to compare experimental and analytical results. The experimental and analytical results were found to correlate better in walls with lower vertical reinforcement ratios in comparison to the walls with higher vertical reinforcement ratios. The moment-curvature analysis was based on flexural behavior and the plane-section assumption. This assumption became invalid for walls with large vertical reinforcement ratios and large shear deformations. The researchers concluded that analytical moment-curvature analysis is not appropriate for walls that experience significant shear deformations.

The test results also verified that properly designed and reinforced masonry shear walls are adequate for seismic resistance as the walls exhibited a sufficient level of ductility and the ability to dissipate energy. Higher levels of ductility were seen in walls dominated by flexural behavior in comparison to walls that failed in shear. However, it was also shown that increased axial load can have the negative impact of changing a mixed flexural/shear failure to a more brittle shear failure. Ductility was significantly decreased in flexural walls with sizeable axial loads due to increased toe spalling and the lack of confinement.

The researchers also concluded that the contribution of horizontal reinforcement to shear strength was inconsistent. The results demonstrated that the formation of the first major diagonal

crack is largely dependent upon the tensile strength of the masonry and not the level of reinforcement. Shear specimens with larger amounts of horizontal and vertical reinforcement did display higher levels of ductility and energy-dissipation, however. Increased amounts of horizontal steel had the effect of changing the failure mechanism of a wall from a brittle shear failure to a ductile flexural failure.

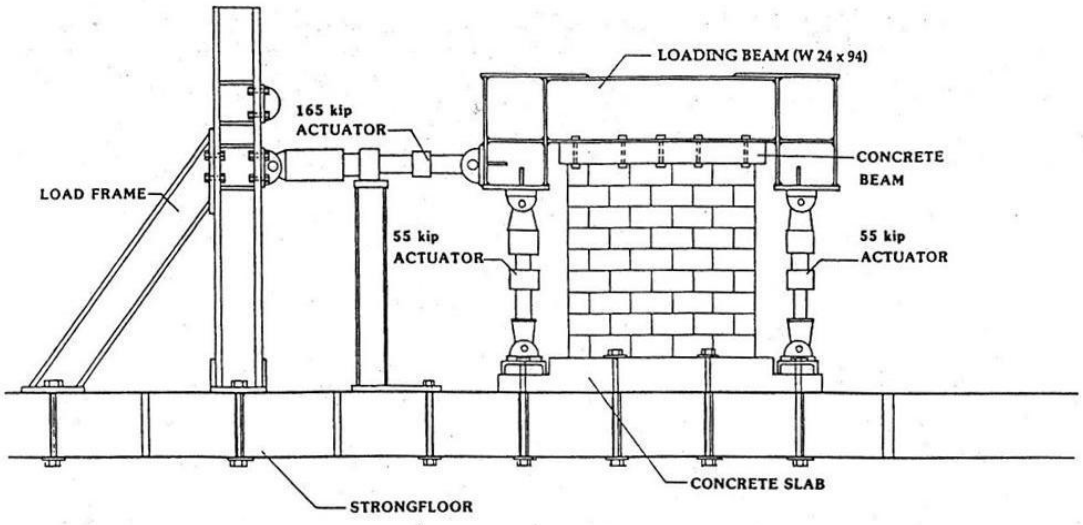

Figure 2.2 Shing et al. – test apparatus and setup

2.3.2 Eikanas

Eikanas (2003) investigated the behavior of concrete masonry shear walls with varying aspect ratios and amounts of flexural reinforcement. The main goal of this research was to investigate the validity of the maximum reinforcement provisions found in the 2000 International Building Code (IBC). Seven fully-grouted concrete masonry walls were constructed and tested as cantilevers. A constant axial stress of approximately 27 psi was applied in each test and cyclic in-plane loads were supplied at the top of each wall. Aspect ratios of 0.72, 0.93, 1.5, and 2.1 were used, and all walls were nominally 8 in. thick with an actual thickness of 7.625 in. The

flexural reinforcement ratio used was either approximately equal to the IBC maximum reinforcement ratio or twice the IBC maximum reinforcement ratio. All horizontal reinforcement consisted of No. 4 bars uniformly distributed at a spacing of 16 in. Properties of the walls tested by Eikanas are presented in further detail in Table 2.1.

Test results demonstrated that squat shear walls (walls with a low aspect ratio) underwent significant deformation due to shear, while taller, slender walls were more prone to flexural deformations. Eikanas also observed that while larger amounts of vertical reinforcement did lead to smaller drift capacities, the drift values were always greater than 1.5% before 20% load degradation was reached. The IBC provisions were found to be excessively restrictive and failed to appropriately consider the aspect ratio of the wall. Eikanas also concluded that the consideration of flexural deformations for squat shear walls was inappropriate as they will largely undergo shear deformations.

Table 2.1 Properties of walls tested by Eikanas

Wall Specimen	Total Height (in.)	Height to Load (in.)	Wall Length (in.)	Aspect Ratio	Horiz. Reinf. # of Bars - Bar # @ o.c. spacing	Vert. Reinf. # of Bars - Bar # @ o.c. spacing
1	72	52	55 5/8	0.93	5 - #4 @ 16"	4 - #5 @ 16"
2	104	84	55 5/8	1.50	7- #4 @ 16"	4 - #5 @ 16"
3	104	84	39 5/8	2.10	7 - #4 @ 16"	3 - #5 @ 16"
4	72	52	55 5/8	0.93	5 - #4 @ 16"	7 - #5 @ 8"
5	104	84	55 5/8	1.50	7- #4 @ 16"	7 - #5 @ 8"
6	104	84	39 5/8	2.10	7 - #4 @ 16"	5 - #5 @ 8"
7	72	52	71 5/8	0.72	5 - #4 @ 16"	5 - #5 @ 16"

2.3.3 Voon and Ingham

Voon and Ingham (2006) performed experimental analysis on the shear strength of reinforced concrete masonry walls. Ten single-story cantilever walls were subjected to an in plane horizontal shear force with cyclic and displacement controlled loading. The test setup is

shown in Figure 2.3. Variables included the amount and distribution of shear reinforcement, type of grouting, aspect ratio, and level of axial stress. Eight walls were tested with an aspect ratio of one (1.8 m in height and length), one wall with an aspect ratio of 2.0 (3.6 m tall), and one with an aspect ratio of 0.6 (1.8 m in height and 3 m in length). Two of the walls were partially grouted as only cells containing reinforcing bars were filled with grout. The partially-grouted walls also contained no horizontal shear reinforcement. For the fully-grouted walls, the horizontal reinforcement ratio varied between 0.01% and 0.14%. Nine of the walls were designed to exhibit a shear failure mechanism and one was designed to fail in flexure. Each wall was tested to failure which was defined as the point on the loading curve where the wall strength had degraded to 80% of the maximum strength previously recorded.

Eight of the walls failed in shear, with one wall exhibiting a mixed flexure/shear failure and another failing due to a combination of flexure and sliding. Results from the wall tests demonstrated that increased axial compression increased the in-plane shear performance of masonry walls. This was attributed to the suppression of tension stresses in the masonry which is inherently weak in tension. Uniformly distributed shear reinforcement was shown to improve the post cracking performance of masonry walls as diagonal cracks were not able to widen as the lateral displacement increased. Higher energy dissipation and higher levels of ductility were observed in walls with adequate and uniformly distributed shear reinforcement. Wall tests demonstrated that masonry shear strength increased with a decrease in aspect ratio and that partial grouting resulted in similar maximum strengths as fully grouting when net area shear stress is considered. The test results also were compared with New Zealand masonry design standard NZS 4230:1990 and it was determined the standards were too conservative. The shear

strength exhibited by the walls substantially surpassed the maximum shear stress allowed by the code.

Displacement ductility values were reported by Voon based upon the displacement corresponding to maximum strength, d_{vmax}, and a yield displacement obtained from an elasto-plastic approximation of the hysteresis envelopes. Lateral forces were measured during the first cycle at ±1 mm displacement and used to obtain an initial stiffness of the approximate system. The yield displacement corresponded to the intersection of the initial stiffness and the predicted flexural strength. Reported displacement ductility values for walls failing in shear ranged from 1.33 to 2.85.

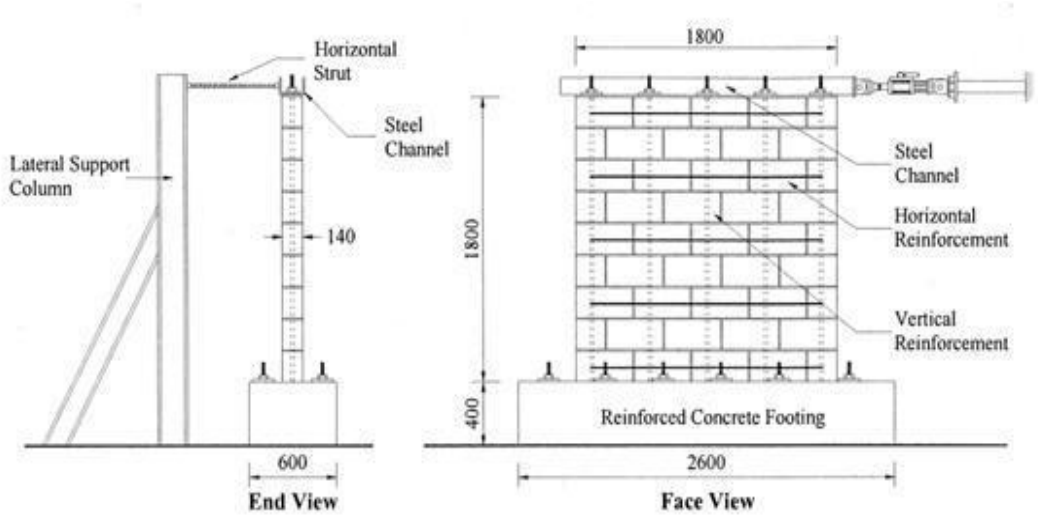

Figure 2.3 Voon and Ingham – test apparatus and setup

2.3.4 Sveinsson et al.

Sveinsson et al. (1985) conducted in-plane shear tests on thirty fully grouted masonry piers involving three different types of masonry construction. Concrete blocks, clay bricks, and a double-wythe, grouted core, clay brick configuration were all tested under fixed-fixed

conditions. Only the concrete block and clay brick masonry walls were investigated as part of this study. All of the test specimens measured 56 in. high and 48 in. wide. The walls were loaded in double bending due to the fixed-fixed end conditions. The test apparatus and setup is shown in Figure 2.4. Due to the double-bending loading conditions, the effective height of each wall was only half of the actual height, resulting in an aspect ratio of 0.58. Variables examined in the study included the level of axial stress, the amount and anchorage of horizontal shear reinforcement, and the distribution of flexural reinforcement.

The majority of the walls failed in either shear or due to a combination of shear and sliding. Only two of the 25 concrete and clay walls failed in flexure. The study indicated increased lateral resistance with increased levels of axial stress. However, high levels of vertical load also led to decreased ductility as the failures became more brittle. Proper anchorage of shear reinforcement by means of a 180° hook was found to enhance strength and create more gradual failures. Also, improved ductility was observed in walls where the shear reinforcement consisted of smaller bar sizes uniformly distributed. Displacement ductility of the piers was not calculated or directly considered.

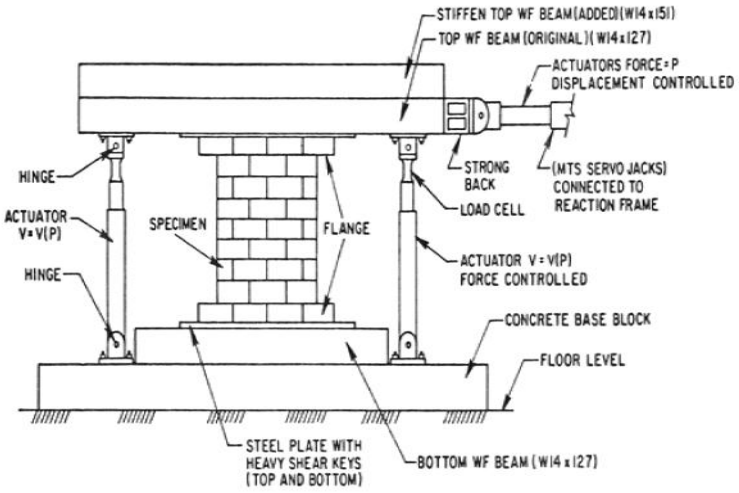

Figure 2.4 Sveinsson et al. – test apparatus and setup

2.3.5 Shedid

Shedid (2008) examined the behavior of reinforced concrete masonry shear walls failing in flexure. Six fully grouted walls were subjected to in-plane cyclic lateral loading. The amount and distribution of vertical reinforcement and the level of axial compression were varied in each specimen to examine the effects on inelastic behavior and ductility. Information on post peak behavior was collected by cycling each wall until a 50% drop in strength occurred. The hysteresis curve obtained from Shedid's first wall test is shown in Figure 2.5. Each wall measured 3.6 m in height and 1.8 m in length for an aspect ratio of 2.0. The high aspect ratio was chosen to ensure flexural behavior with a definitive region of plastic hinging. The walls were constructed with 190 x 190 x 390 mm concrete masonry blocks and horizontal reinforcement for each wall consisted of a No. 10 bar (100 mm^2 area) at a uniform spacing of either 600, 400, or 200 mm. Adequate amounts of horizontal reinforcement were provided in order to ensure a ductile flexural failure and to prevent against a brittle shear failure. The vertical reinforcement ratio varied between 0.29 and 1.31.

Shedid measured displacements at several different steps in the testing of the wall specimens in order to consider different definitions of yield and ultimate displacement in the calculation of displacement ductility. Ultimate displacements were measured corresponding to maximum load, 1% drift, and to the point at which strength had degraded to 80% of the maximum previously reached. Various yield displacement measurements were also considered including the displacement at the first yield of the outermost vertical bar and various elastic-plastic approximations (see Figure 2.8).

Shedid observed that the displacement ductility was decidedly dependent on the amount of vertical reinforcement. Larger vertical reinforcement ratios resulted in lower ductility values

due to the fact that the yield displacement tended to increase with higher levels of vertical reinforcement while the displacements observed at maximum load were similar for all six walls. Increased axial compressive stress also caused a slight decrease in the displacement ductility. Overall the test walls demonstrated that reinforced masonry shear walls failing in flexure exhibit adequate ductile behavior, considerable energy dissipation, and little strength degradation up to and beyond commonly used drift levels.

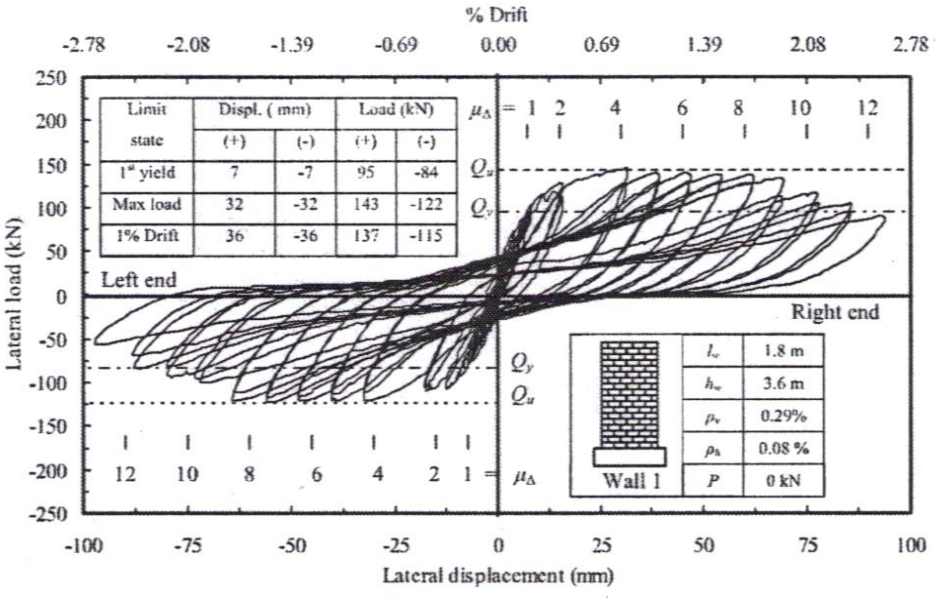

Figure 2.5 Typical hysteresis curve from Shedid (2008)

2.3.6 Snook

Snook (2005) investigated the strengthening effect of confinement reinforcement in masonry shear walls. Various confinement reinforcement schemes were used: steel confinement plates, seismic combs, and polymer fibers mixed into the grout. Nine cantilever walls were tested with two of the walls being unconfined in order to serve as a baseline. In-plane cyclic loading and constant axial load were applied to all walls. The flexural reinforcement was held

constant for all test specimens while the shear reinforcement varied between either a No. 4 or No. 5 bar at 16 in. on center.

Displacement ductility was reported by Snook (2005) using an ultimate displacement based on 20% load degradation at failure. Yield displacement was determined using a line from the origin and through the point of first yield of extreme reinforcement up to the theoretical yield force. The bilinear approximation used by Snook is given in Figure 2.6. Reported ductility values varied between 4.1 and 7.3 with the higher values seen in the confined specimens.

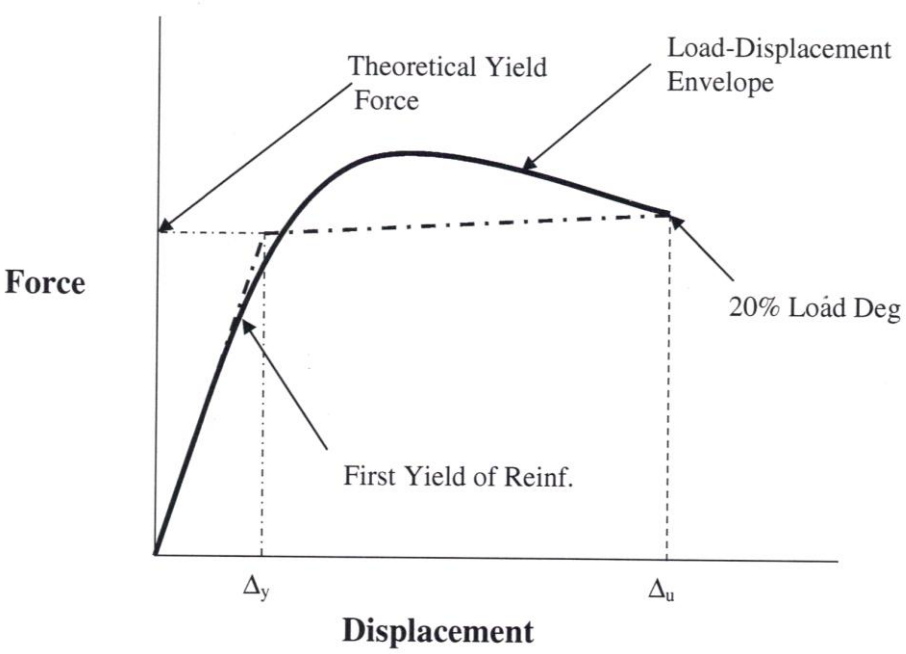

Figure 2.6 Bilinear approximation used by Snook (2005)

Confinement reinforcement increased the in-plane performance of the shear walls. The greatest impact was seen on the walls' capacity for energy absorption and displacement ductility. Minor increases were also observed in drift capacity. Confinement in the form of grout fiber reinforcement was the most effective confinement method and resulted in the largest increases in performance compared to that for the unconfined specimens.

2.3.7 Priestley

Priestley (1986) examined the seismic design of concrete masonry shear walls based upon two different previous experimental studies of such walls under cyclic in-plane loading. Priestley argued that elastic design methods are inappropriate for design of masonry under seismic loading and that ultimate strength methods should be used instead. Ultimate strength of masonry should be considered because elastic design of masonry will not prevent inelastic behavior during a seismic event and because a structure's behavior at ultimate loads is as predictable as behavior seen at service loads. Thus Priestley argued that it was more realistic to recognize that the ultimate capacity of the masonry structure will be achieved and to design appropriately to ensure proper ductility without rapid strength degradation.

The first experimental study Priestley participated in examined the seismic resistance of reinforced concrete masonry shear walls with high steel percentages. Six heavily reinforced and fully grouted walls were subjected to cyclic loading to investigate the effects of variables such as the amount of steel reinforcement, influence of axial stress, and inclusion of confining steel plates in the bottom three mortar courses. An aspect ratio of 0.75 was maintained in all walls. Ductile behavior was achieved in all specimens but significant load degradation occurred due to the wall sliding along the top of the foundation beam. The results demonstrated that flexural failure modes could be achieved from squat walls but that energy dissipation was limited by base slip.

Experimental studies were also conducted on slender cantilever masonry shear walls measuring 19.7 ft in height and with an aspect ratio of 2.5. Three fully grouted concrete masonry walls were subjected to in-plane cyclic loading to investigate the influence of aspect ratio on ductility capacity, the use of confining plates in the plastic hinge region, and the potential for

buckling of the compression end of the plastic hinge region. Confining steel plates were used in only one of the test specimens and were placed at each end of the wall within the second and eighth mortar courses.

Results from the testing of the slender walls demonstrated that the confinement in the plastic hinge region improved both the strength and ductility of the walls. The walls without confinement also experienced higher levels of damage at the end of testing in comparison to the confined wall. Lapping of flexural reinforcement in the plastic hinge region resulted in bond failure and higher compression strains at an earlier stage of testing than anticipated. As a result, Priestley recommended that lap splices be avoided in potential plastic hinge zones. No lateral buckling was observed during testing even after spalling of face shells. Also, the ductility capacity was reduced with increased aspect ratio confirming a prior theoretical prediction.

2.4 Ductility

In regions of moderate to high seismic activity, it is not economical to design structures to remain elastic as the design forces will be extremely high. As a result, structures must be designed to undergo inelastic deformations without suffering failure or collapse. Ductility is commonly considered as a parameter in seismic design because it demonstrates the ability of a structure to maintain strength under inelastic deformation. Priestley (2007) defines ductility as the ratio of maximum to effective yield deformation. Different measures of deformation can be considered such as displacement or curvature. Displacement ductility (the ratio of ultimate displacement to yield displacement) is generally the most convenient form of ductility to evaluate, making it one of the most commonly referenced parameters in the seismic design and assessment of structures.

2.4.1. Definitions of Yield and Ultimate Displacement

In elastic-perfectly plastic systems the displacement ductility, μ_Δ, is defined as

$$\mu_\Delta = \frac{\Delta_u}{\Delta_y} \tag{2-1}$$

where Δ_y is the displacement at the onset of yield and Δ_u is the displacement at a predetermined definition of failure. The yield and ultimate displacements in the elasto-plastic system are shown in Figure 2.7. The definition of yield displacement (Δ_y) and the definition of failure at which the ultimate displacement (Δ_u) is determined have not reached a consensus within the seismic research and design community, and several definitions may be used in consideration of displacement ductility.

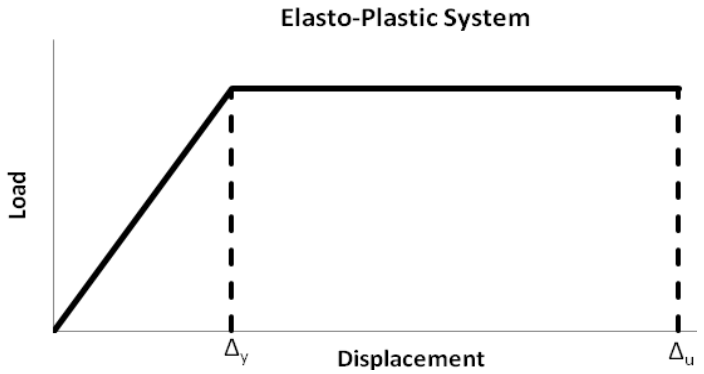

Figure 2.7 Yield and ultimate displacements in the elasto-plastic system

Unlike in elastic-perfectly plastic systems, the yield limit is not well defined for masonry walls, as walls with different features may exhibit various yield mechanisms. Therefore it is common to create an equivalent elasto-plastic or bilinear system for each masonry wall's load-displacement history. The yield displacement is then taken from this equivalent system. This method also varies, however, and several options exist when defining the yield of the chosen equivalent system.

In one simplified process, the actual yield displacement may be used which is typically based on the first onset of yielding recorded in the extreme vertical reinforcement of the masonry wall. In other cases, Δ_y may be defined as the yield displacement corresponding with the point where extension of the elastic line through the actual yield point reaches the maximum load. Another method used is to define an effective Δ_y as the value that produces equal energy under the curves up to a determined failure level such as 20% strength degradation or 1% drift (Shedid, 2008). See Figure 2.8 for various yield and ultimate displacements considered by Shedid (2008). Yet another method to determine the yield displacement utilizes the theoretical moment capacity and theoretical yield force of the wall. A line is extrapolated from the origin through the point of measured first yield of extreme reinforcement to the theoretical yield force. The point of intersection between the extrapolated line and theoretical yield force provides the yield displacement (Snook, 2005).

The definition of the ultimate displacement can also vary and is largely dependent upon the definition of failure that is used. In some cases the post peak capacity of the wall is ignored, and the ultimate displacement is defined as the displacement corresponding with the maximum load. In other cases, a specific limit on displacement is placed (typically 1% drift) where it is argued that additional ductility beyond that point cannot be utilized (Shedid, 2008). Ultimate displacement would then be defined as the displacement corresponding to 1% drift. More commonly, however, the ultimate displacement is based upon recognition of the fact that considerable strength still exists even after degradation has begun. In this case the ultimate displacement is often defined as the displacement corresponding to 80% of the maximum strength reached during testing. Shing et al. (1991) considered an ultimate displacement

corresponding to 50% strength degradation in calculating displacement ductility of 16 fully grouted masonry walls subjected to cyclic in-plane loading.

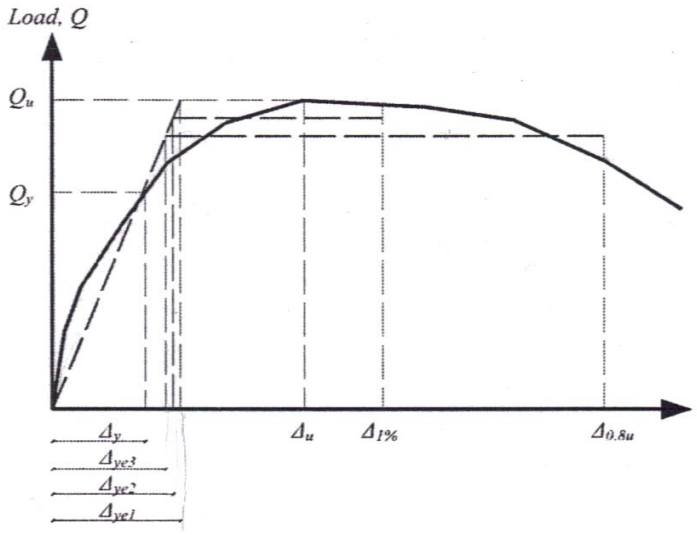

Figure 2.8 Various yield and ultimate displacement definitions considered in determining displacement ductility (μ_Δ) (Shedid, 2008)

2.4.2 Paulay and Priestley

In the book *Seismic Design of Reinforced Concrete and Masonry Structures* by Paulay and Priestley (1992), the authors conclude that structures in seismic areas with moderate resistance to lateral forces must be able to minimize significant damage and protect against structural failure or collapse. The structure must be capable of sustaining much of its initial strength when large deformations beyond the elastic limit are caused by seismic activity. Ductility is the structure's ability to maintain strength in the inelastic domain of response. It is characterized by both the ability to withstand sizeable deformations and the ability to dissipate energy through hysteretic behavior. As a result, the authors conclude that ductility is "the single most important property sought by the designer of buildings located in regions of significant seismicity" (Paulay and Priestley, 1992).

Inelastic deformations of cantilever walls and the formation of a plastic hinge zone were also considered. Large inelastic curvatures and plastic yielding of vertical reinforcement occur at the base of the wall in what is known as the plastic hinge. The curvature over a cantilever wall is not linear due to the formation of the plastic hinge and the authors present an elastic region and a plastic region to idealize the curvature profile. Similarly the total deflection of the cantilever consists of a yield or elastic component and a fully plastic component. Plastic rotation was considered to act at mid-height of the equivalent plastic hinge and an equation relating displacement ductility to wall height (h_w), curvature ductility (μ_φ), and equivalent plastic hinge length (l_p) was presented as seen in Equation 2.2.

$$\mu_\Delta = 1 + 3\left(\mu_\varphi - 1\right)\frac{l_p}{h_w}\left(1 - 0.5\frac{l_p}{h_w}\right) \tag{2-2}$$

For masonry cantilever walls with rectangular sections, the authors approximate the plastic hinge length as half the wall length. This simplifies Equation 2.2 to

$$\mu_\Delta = 1 + \frac{3}{2A_r}\left(\mu_\varphi - 1\right)\left(1 - \frac{1}{4A_r}\right) \tag{2-3}$$

where A_r is the wall aspect ratio (ratio of wall height to wall length). The curvature ductility, (ratio of yield curvature to ultimate curvature) will be constant for a given wall length and axial load. Thus the authors argue that the available displacement ductility decreases as the aspect ratio increases. Additionally the authors present design charts and research data indicating that the ductility of rectangular masonry walls decreases as axial load, reinforcement ratio, or reinforcement yield stress increase. Ductility capacity is increased through increases in masonry compression strength and the use of confinement.

The theoretical length of the plastic hinge was also examined by the authors as the curvature ductility is greatly affected by the plastic hinge length. The authors found that

theoretically the plastic hinge length was directly proportional to the wall length. These theoretical predictions did not match well with experimentally measured plastic hinge lengths however. The authors attributed this to the elongation of tensile flexural bars into the footing which produced additional rotation and deflection and was not considered in the theoretical approach. Also flexure-shear cracking resulted in higher steel strains above the base than what was predicted by the bending moment. The authors suggested a new equation for estimation of the plastic hinge length based on wall height and size and strength of reinforcement.

$$l_p = 0.08h_w + 0.15d_b f_y \ (ksi) \tag{2-4}$$

Paulay and Priestley (1992) also examined the use of bilinear models to approximate load displacement behavior and the interpretation of yield and ultimate displacements. The bilinear approximation used by the authors (see Figure 2.9) utilizes an idealized linear elastic response based upon a line passing through the origin and 0.75 times the yield strength of the real load-displacement curve. The yield displacement is determined from the intersection of the idealized linear elastic response and the horizontal line at yield strength. The ultimate displacement is based upon 20% strength degradation in the load displacement curve.

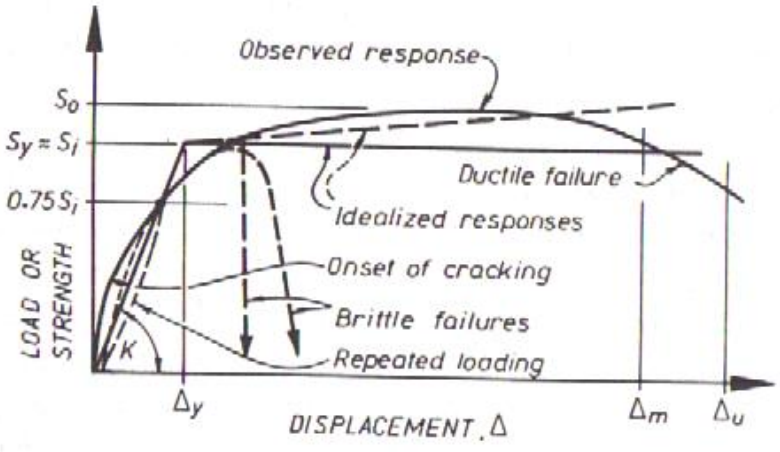

Figure 2.9 Bilinear approximation considered by Paulay and Priestley (1992)

2.4.3 Priestley and Kowalsky

Priestley and Kowalsky (1998) derived equations for ductility and drift capacity of rectangular concrete cantilever shear walls based upon moment-curvature analyses that showed the insensitivity of wall curvatures to different parameters. Analyses were based on walls with the dimensions and material properties held constant. The axial load compression stress was varied in the range of 0 to 3.0 MPa, and the longitudinal reinforcement ratio was varied between 0.25% and 2.0%. A uniform distribution of reinforcement was considered as well as a distribution that concentrated much of the reinforcement at the ends of the wall. The yield, serviceability, and ultimate curvatures (as defined by the authors) were shown to be relatively unaffected by the variations in axial load, longitudinal reinforcement ratio, and distribution of longitudinal reinforcement.

Values of yield, serviceability, and ultimate curvature were obtained from the analyses that were independent of the tested parameters. The yield curvature was defined as a function of wall length alone, for a given steel yield stress. Serviceability and ultimate curvatures were dependent only on the wall length. The authors observed that the independence of the yield curvature from the axial load ratio and longitudinal reinforcement ratio implied that yield deflection is also independent of axial load and reinforcement content. An equation for the yield displacement was introduced based upon the yield strain of the reinforcement, the effective height of the wall, and the length of the wall.

The moment-curvature analyses indicated that the yield, serviceability, and ultimate curvatures could be expressed as constant values, and thus the curvature ductility (μ_φ) at serviceability and ultimate states could also be considered constant. Equations from Paulay and Priestley were presented for prediction of the plastic hinge length, l_p. Estimates of the

displacement ductility capacity of a wall were then found in relation to the curvature ductility capacity using Equation 2-2. Wall displacement ductility capacity was shown to reduce with increases in aspect ratio.

Estimates of drift capacity at the ultimate state were also considered. Once again the constant curvature values found from the moment-curvature analyses were utilized. A linear curvature distribution along the height of the wall was assumed and equations for the elastic and plastic drift angle were derived. The total maximum drift was found by summing the elastic and plastic contributions. Results from these estimations showed that the New Zealand code drift limits would govern for the design of walls of even very low aspect ratios.

2.4.4 Ayers

Ayers (2000) expanded on the work of Priestley and Kowalsky (1998) by determining dimensionless relationships for curvature in rectangular masonry walls. Ayers utilized moment-curvature analyses of 16 masonry walls to explore the effects of certain variables on curvature relationships. The level of axial load and amount of reinforcement were varied, but the reinforcement was uniformly distributed in all cases. Concrete block and clay brick masonry walls were considered as well as confined and unconfined arrangements. Curvature was assessed at the three limit states evaluated by Priestley and Kowalsky (1998): yield, serviceability, and ultimate. Given a specified wall length, constant relationships were established for the yield and serviceability curvatures and a linear relationship was found for the ultimate curvature.

Based on the results of the moment curvature analyses, Ayers proposed equations for the yield curvature of unconfined concrete block, unconfined clay brick, confined concrete block,

and confined clay brick walls. The moment-curvature analyses showed that yield curvature was essentially independent of the axial load and amount of longitudinal reinforcement. As a result, the proposed equations for yield curvature were dependent only on the wall length and yield strain of the longitudinal reinforcement. Priestley (2007) generalized the results of Ayers study and recommended using one equation for the yield curvature of both clay brick and concrete block unconfined masonry. The proposed yield curvature equation from Priestley is seen below as Equation 2-5.

$$\varphi_y = \frac{2.1\varepsilon_y}{l_w} \tag{2-5}$$

The ultimate limit state considered in the study was based on values of the ultimate compressive strain in the masonry. The strain values used were 0.003 for unconfined concrete block, 0.004 for unconfined clay brick, and 0.008 for confined clay brick and concrete block. Ayers noted that these strains were conservative as they were based on design values of ultimate strain.

The ultimate curvature was determined to be a function of the longitudinal or vertical reinforcement ratio given a defined wall length. For unconfined concrete block masonry:

$$\varphi_u = \frac{-12.623\rho_v + 29.07925}{1000 l_w} \tag{2-6}$$

For unconfined clay brick masonry:

$$\varphi_u = \frac{-16.512\rho_v + 36.899}{1000 l_w} \tag{2-7}$$

Ayers also presented charts to determine the ultimate curvature at masonry compressive strains and steel tensile strains greater than those considered in the ultimate state defined in the study. The charts were created to enable engineers to design a wall to a specific masonry or steel strain instead of just the strains considered in the earlier analysis. It should also be noted that Ayers'

work assumed that the walls behaved in a flexural manner and did not take into account walls controlled by shear or sliding.

2.5 MSJC Code Provisions (2008)

The Masonry Standards Joint Committee (MSJC) *Building Code Requirements and Specification for Masonry Structures* (MSJC, 2008*)* includes provisions for seismic design in Section 1.17. Provisions are laid out for three different classifications of reinforced masonry shear walls: ordinary, intermediate, and special. The various wall types are intended to have different capabilities for inelastic response and energy dissipation during a seismic event. Prescriptive requirements are provided in the form of minimum cross-sectional areas of horizontal and vertical reinforcement and a limit on the maximum spacing of the reinforcement. These requirements are presented to ensure that the "minimum level of assumed inelastic ductility" is available.

The minimum reinforcement requirements for ordinary reinforced masonry walls are found in Sections 1.17.3.2.3.1 and 1.17.3.2.4. The maximum spacing for horizontal and vertical reinforcement is 120 in. The minimum cross-sectional area of reinforcement is 0.2 $in.^2$ (equivalent to one No. 4 bar) for both horizontal and vertical reinforcement. Ordinary reinforced masonry shear walls are allowed in areas of low and moderate seismic risk and are permitted in Seismic Design Categories (SDC) A, B, and C.

Prescriptive reinforcement provisions for intermediate reinforced masonry shear walls (Section 1.17.3.2.5) are largely the same as for ordinary walls but the spacing between vertical reinforcement is reduced to 48 in. These walls have more favorable seismic design parameters than ordinary walls, namely a higher response modification factor, R. Intermediate reinforced

masonry shear walls are allowed in areas of low and moderate seismic risk and are permitted in SDC A, B, and C.

Spacing and minimum reinforcement requirements for special reinforced masonry shear walls (Section 1.17.3.2.6) are more restrictive with the intent to improve performance in the inelastic range of behavior. For vertical reinforcement, the spacing requirements are modified from those seen in intermediate walls to:

$$s_{max} \leq 48\ in., \frac{l_w}{3}, \frac{h_w}{3}$$ (Running bond)

Or $s_{max} \leq 24\ in.$ (Other than running bond)

The minimum cross-sectional area of vertical reinforcement must be greater than or equal to one-third of the required shear reinforcement. Additionally, the sum of the cross-sectional area of horizontal and vertical reinforcement must be at least 0.002 multiplied by the gross cross-sectional area of the wall.

The MSJC establishes a minimum level of in-plane shear reinforcement to improve ductility in special walls in Sections 1.17.3.2.6(a) through 1.17.3.2.6(e). Horizontal reinforcement in special reinforced masonry shear walls is required to resist in-plane shear and must be uniformly distributed and embedded in grout. It must also be anchored appropriately using standard hooks around vertical reinforcing bars. The maximum spacing allowed for horizontal reinforcement is the same as that allowed for vertical reinforcement. Special reinforced masonry shear walls are permitted to be used as part of the system that resists earthquake loading in any SDC. The reinforcement requirements for all three wall types are summarized in Table 2.2.

Additional shear capacity design provisions for special reinforced masonry shear walls are found in Section 1.17.3.2.6.1. These provisions are in place to enhance ductility by attempting to eliminate the occurrence of shear failures prior to achieving inelastic flexural wall behavior. For walls being designed in compliance with strength design, the design shear strength must exceed the shear corresponding to the development of 1.25 times the nominal flexural strength of the wall. The nominal shear strength is capped, however, and need not exceed 2.5 times the required shear strength. Special reinforced walls being designed under ASD provisions utilize a different approach to protect against shear failures. In this case, the shear or diagonal stress resulting from in-plane seismic forces must be increased by a factor of 1.5. The 1.5 factor does not apply to the overturning moment acting on the wall however. Once again the intent of the provision is to increase the ductile performance of the wall by making the flexure mode of failure more dominant.

In Section 3.3.3.5, for strength design, the maximum area of flexural tensile reinforcement is also restricted for each of the three wall types. This is done to ensure that the compressive zone of the masonry does not begin to crush before an adequate level of ductility is reached. A sufficient level of ductility is ensured by monitoring the tensile strain in the flexural reinforcement. An adequate level of post-yield strain (consistent with the ductility implied in the wall design) must be developed in the extreme flexural reinforcement of the wall. The desired amount of tensile strain is provided by a tensile strain factor which varies accordingly with the amount of curvature ductility anticipated. Ordinary walls are assigned a tensile strain factor of 1.5, intermediate walls a factor of 3, and special walls are assigned the largest factor of 4 as they are designed to have the highest ductility. This means that the amount of flexural reinforcement in a special wall must be limited such that the tensile strain developed in the extreme flexural

reinforcement will be at least four times its yield strain prior to the compressive zone reaching its ultimate strain (a compressive strain of 0.0025 for concrete and 0.0035 for clay masonry).

Table 2.2 Reinforcement requirements for MSJC 2008 wall types (Adapted from Shedid, 2006)

<table>
<tr><th rowspan="3">Wall Type</th><th colspan="4">Reinforcement Requirements</th></tr>
<tr><th colspan="2">Horizontal</th><th colspan="2">Vertical</th></tr>
<tr><th>Min. amount</th><th>Max. spacing</th><th>Min. amount</th><th>Max. spacing</th></tr>
<tr><td rowspan="2">Ordinary</td><td>0.2 in.^{2} in Bond Beam</td><td>120 in.</td><td rowspan="2">0.2 in^2</td><td rowspan="2">120 in.</td></tr>
<tr><td>2 W1.7 wires as joint reinforcement</td><td>16 in.</td></tr>
<tr><td rowspan="2">Intermediate</td><td>0.2 in.^{2} in Bond Beam</td><td>120 in.</td><td rowspan="2">0.2 in^2</td><td rowspan="2">48 in.</td></tr>
<tr><td>2 W1.7 wires as joint reinforcement</td><td>16 in.</td></tr>
<tr><td rowspan="2">Special</td><td>0.2 in.^{2} in Bond Beam</td><td>Lesser of: 48 in. or (1/3)H or (1/3)L</td><td rowspan="2">1/3 of required shear reinforcement</td><td rowspan="2">Lesser of: 48 in. or (1/3)H or (1/3)L</td></tr>
<tr><td>2 W1.7 wires as joint reinforcement</td><td>16 in.</td></tr>
</table>

CHAPTER 3

ASSESSING DUCTILITY AND DRIFT

3.1 Introduction

Displacement ductility and drift are important parameters in the seismic design of structures, and there has been recent interest from both researchers and designers about the values of ductility and drift that can be achieved by each MSJC wall type. In this study, ductility and drift values were determined from test results for 67 fully-grouted concrete and clay masonry walls obtained from six different studies: Sveinsson et al. (1985), Shing et al. (1991), Eikanas (2003), Snook (2005), Shedid (2006) and Voon and Ingham (2006). Data from the wall tests are given in Appendix A. Wall studies selected were restricted to single-story uncoupled walls to simplify analysis and ensure comparable behavior. All experimental studies subjected walls to in-plane cyclic lateral loading and utilized displacement-controlled testing. Displacement was increased in each study until a predefined level of failure was reached. The majority of the walls were tested as cantilevers, but walls emulating fixed-fixed conditions were also evaluated.

Two different sets of data were compiled for walls failing in either flexure or shear. After determining displacement ductility and drift, the walls were classified according to the 2008 MSJC provisions for special, intermediate and ordinary shear walls as given in Section 1.17 and in the strength design section (Section 3.3.3.5). Further analysis of the walls examined the relationship of displacement ductility, drift, and wall classification to a number of parameters, including aspect ratio, horizontal reinforcement ratio, vertical reinforcement ratio, and axial stress.

In this chapter, the procedures used in interpreting test parameters and in determining wall types are presented. Interpretation of displacement ductility and drift is explained in Section 3.2. The procedure used to classify the 67 shear walls into MSJC wall types is presented in Section 3.3, and interpretation of other test parameters is presented in Section 3.4. Section 3.5 describes the procedures used to calculate theoretical values of displacement ductility, yield displacement, and ultimate displacement for walls failing in flexure.

3.2 Interpretation of Displacement Ductility and Drift

The definition of yield and ultimate displacement used to determine displacement ductility has not reached a consensus within the seismic research and design community. Consequently, various definitions were presented in the previous studies of the in-plane performance of masonry shear walls. In order to facilitate the evaluation of displacement ductility, consistent definitions of yield and ultimate displacement were established.

All of the yield displacements reported in this study are based upon a bilinear approximation. Yield displacements were taken directly from their respective studies for walls tested by Shedid (2008), Voon (2007), and Shing et al. (1991). In studies where yield displacement was not considered or was not based upon a bilinear approximation, the yield displacement was taken from the load-displacement envelope or hysteresis curve. The yield displacement in this case was based upon a bilinear approximation similar to the technique presented by Shing et al. (1991). The linear elastic range was represented by a line through the origin and a point at 50% of the maximum lateral load on the actual load displacement or hysteresis curve. This line was extended up to a horizontal line at the maximum lateral load for the test. The yield displacement was defined at the intersection of the max lateral load line and

the extended linear elastic line. In cases where the hysteresis curve was used, the yield displacement was determined as the average value from both directions of loading.

The ultimate displacement used in the calculation of displacement ductility was defined as the displacement corresponding to a 20% strength degradation of the test specimen. After the maximum lateral load, V_u, had been reached and the strength of the specimen began to degrade, the ultimate displacement was found corresponding to 80% of V_u. In some studies this displacement was reported directly, while in others it was determined from the load displacement envelope or hysteresis curve. The average ultimate displacement between the two directions of loading was used if the ultimate displacement was obtained from the hysteresis curve.

An ultimate displacement definition of 20% strength degradation was selected because it demonstrates the considerable strength maintained by a specimen even after reaching peak load. All of the walls classified were subject to this definition of ultimate displacement with the exception of the concrete block and clay brick walls tested by Sveinsson et al. (1985). In that study, the wall tests were ended following a sharp drop in shear strength and excessive opening of significant diagonal cracks. Due to this definition of failure, almost all of the wall tests ended prior to reaching 20% strength degradation. Thus, for these tests, the ultimate displacement was taken as the reported maximum displacement prior to failure.

Drift was defined as the ratio of ultimate displacement to overall wall height. The same definition of ultimate displacement that was used in determining displacement ductility was used in determining drift. In the case of the fixed-fixed wall tests, the overall wall height was used in determining drift.

Wall tests used in the analysis were restricted to those walls for which sufficient data was available to determine both displacement ductility and drift. Essentially each individual wall test

had to be represented in either a load displacement envelope or hysteresis curve in order to be considered. Displacements were then taken from the load displacement curve or hysteresis curve accordingly. In some cases, displacements at notable events in the wall test were noted and presented in the respective experimental study. If the reported displacements were in accordance with the definitions of displacements used in this study, then they were taken directly from the study and used in the calculation of displacement ductility and drift.

3.3 Interpretation of 2008 MSJC Wall Classifications

All 67 fully-grouted reinforced masonry shear walls from the previous experimental studies were classified according to the shear wall types defined in the 2008 MSJC (ordinary, intermediate and special). Classification was based on provisions found in the seismic design section (Section 1.17) and in the strength design section (Section 3.3.3.5). Initial wall classifications were based on the prescriptive reinforcement requirements found in Section 1.17. A given wall had to meet both the amount of reinforcement and spacing requirements in order to satisfy the prescriptive provisions. Classification as a special wall was limited in most cases by the spacing requirement due to limited lengths or heights of test walls. The maximum spacing in these cases became one third of the wall height or length which was restrictive when walls were short in length or height.

The MSJC requires a minimum cross sectional area of horizontal and vertical reinforcement of 0.2 in^2 for all three wall types: ordinary, intermediate, and special. In some walls, the minimum cross-sectional area of reinforcement was not met despite spacing requirements being met or exceeded. This commonly occurred in the form of a No. 3 bar being used as horizontal reinforcement. In order to include more walls in the data set, reinforcement in

walls not meeting the required minimum cross-sectional area was examined on an "average" basis. The required cross-sectional area of reinforcement per unit length of spacing for special, intermediate, and ordinary walls was compared to the actual cross-sectional area of reinforcement per unit length of spacing and classified accordingly.

The last step in the classification of a masonry wall was to check that it complied with maximum flexural reinforcement provisions set in Section 3.3.3.5. Walls with large amounts of reinforcement may result in crushing of masonry prior to adequate development of tensile reinforcement strain and thus limits ductility. In order to check the provisions of 3.3.3.5, a moment-curvature analysis was performed for each wall using the program XTRACT. Strain values in the extreme tensile reinforcement and in the compressive masonry were examined. At a masonry ultimate compressive strain of 0.0025 for concrete masonry or 0.0035 for clay masonry, the strain in the extreme tensile reinforcement was assessed. If the strain in the extreme tensile reinforcement at the time of masonry failure did not meet or exceed the provisions set in Section 3.3.3.5, then the wall was downgraded to a lower wall type. In order to be classified as a special reinforced masonry shear wall, the strain in the extreme tensile reinforcement had to be equal to or exceed four times its yield strain. In intermediate walls the extreme tensile reinforcement strain had to equal or exceed three times the yield strain, and in ordinary walls the strain had to equal or exceed one and a half times the yield strain. The provisions of 3.3.3.5 moved some walls from a special classification to an intermediate or ordinary classification and some intermediate walls to an ordinary classification.

Wall failure modes were taken directly from the interpretation given by the respective authors of each study. Any wall that was classified to have a significant flexural failure mode (including walls exhibiting failure due to a mixture of shear/flexure, sliding/flexure, etc.) was

classified as a flexural failure. The walls classified as shear failures in this study were originally reported by their respective author as failing either due to shear alone or due to a mixed shear/sliding mechanism.

3.4 Interpretation of Other Parameters

After completing displacement ductility calculations, drift calculations and wall classifications, plots were produced to isolate the effects of individual specimen parameters. These plots demonstrated the relationship between a particular variable and displacement ductility or drift. The ratio of the experimental strength of the wall to the calculated nominal strength of the wall (M_{exp}/M_n or V_{exp}/V_n) was also determined. Other parameters investigated include aspect ratio (A_r), horizontal reinforcement ratio (ρ_h), vertical reinforcement ratio (ρ_v), and axial stress (σ_n).

3.4.1 Interpretation of Nominal and Experimental Capacities

The nominal shear capacity, V_n, of each wall was calculated in accordance with strength design shear provisions found in Section 3.3.4.1.2 of the 2008 MSJC. Davis (2008) provided a review of various shear design provisions by calculating the nominal shear capacity of 56 different masonry walls. The 2008 MSJC strength design provisions were found to be the most accurate. The experimental shear capacity of each wall (V_{exp}) was interpreted as the peak lateral load achieved in the experimental study.

Nominal moment capacity M_n, of each wall was calculated using moment-curvature analysis from the program XTRACT. The experimental moment capacity (M_{exp}) was determined by multiplying the peak lateral load by the effective height of the wall. P-Δ effects were not

considered in calculation of the experimental moment as in most cases the increased moment was negligible. For fixed-fixed tests, the walls were loaded in double bending producing an effective height that was half the actual wall height. Cantilever wall tests were only subjected to single bending, and the effective height was equal to the actual wall height.

3.4.2 Interpretation of ρ_v, ρ_h, σ_n, and A_r

The horizontal and vertical reinforcement ratios (ρ_v and ρ_h, respectively) were calculated as the ratio of total cross-sectional area of reinforcement to the gross cross-sectional area of the wall. The level of axial compressive stress (σ_n) was generally reported directly in each respective study. In some cases, the axial load was reported and the axial compressive stress was then calculated as the axial load divided by the gross cross-sectional area of the wall. The aspect ratio (A_r) was calculated as the ratio of effective wall height to wall length.

3.5 Calculation of Theoretical Ductility and Displacements

Equations derived by Paulay and Priestley (1992) and Ayers (2000) made it possible to calculate the theoretical ductility capacity of walls failing in flexure. The yield and ultimate curvatures were calculated using Equations 2-5 through 2-7 as appropriate. From these results, the curvature ductility (μ_φ) was calculated as the ratio of ultimate to yield curvature. Following the same procedure as Ayers (2000), the plastic hinge length was taken to be the greatest of three equations proposed by Paulay and Priestley (1992). The three plastic hinge length equations are:

$$l_p = 0.2l_w + 0.044h_e \tag{3-1}$$

$$l_p = 0.08h_e + 0.022f_y d_b \ (MPa) \tag{3-2}$$

$$l_p = 0.044f_y d_b \ (MPa) \tag{3-3}$$

where l_w is the length of the wall, h_e is the effective height, f_y is the yield strength of the longitudinal reinforcement in MPa, and d_b is the diameter of the reinforcing bars. Using consistent units, the values of plastic hinge length and curvature ductility were then substituted into Equation 2-2 to determine the theoretical displacement ductility. The effective height was used in place of the full wall height for the two fixed-fixed walls failing in flexure from Sveinsson et al. (1985).

The theoretical yield and ultimate displacements were also calculated using equations presented by Paulay and Priestley (1992) and Ayers (2000). The theoretical yield displacement was taken as:

$$\Delta_{y,th} = \frac{\varphi_y {h_e}^2}{3} \tag{3-4}$$

The ultimate displacement was calculated as the sum of the elastic and plastic displacements with the elastic displacement being equal to the yield displacement.

$$\Delta_{u,th} = \Delta_{y,th} + \Delta_p \tag{3-5}$$

The plastic displacement was calculated using equation 3-6.

$$\Delta_p = (\varphi_u - \varphi_y) l_p (h_e - 0.5 l_p) \tag{3-6}$$

The theoretical displacement ductility can also be calculated as the ratio of theoretical ultimate displacement to theoretical yield displacement. Equation 2-2 is only a rearrangement of theoretical ultimate displacement over theoretical yield displacement.

3.6 Summary

In this chapter, the procedures used to calculate experimental displacement ductility and drift for 67 masonry shear walls was presented. Additionally, the classification procedure for shear walls by MSJC wall type and interpretation of other test parameters was defined. The

method used to calculate theoretical yield displacements, ultimate displacements, and ductility of walls failing in flexure was also presented. The calculated values and classifications are used in the following chapter to evaluate the performance of masonry wall and the influence of individual parameters.

CHAPTER 4

EVALUATION OF MASONRY WALL PERFORMANCE

4.1 Introduction

In this chapter, the performance of masonry shear walls under cyclic lateral loading is evaluated using the data compiled from six previous experimental studies. The procedures from Chapter 3 are incorporated to classify walls and to calculate ductility, drift, and other test parameters. Tables representing the statistical evaluation of the data and plots isolating the effects of individual parameters are presented. All wall test data and calculated values are given in Appendix A. The chapter is organized into two main sections: walls failing in flexure and walls failing in shear.

4.2 Evaluation of Performance - Masonry Shear Walls Failing in Flexure

The performance of walls failing in flexure is assessed in the following section by means of statistical evaluation of calculated experimental ductility and drift values. The effects of individual parameters on ductility and drift are also evaluated. In addition, the experimental ductility and displacement values are compared to the theoretical values obtained using the procedures given in Section 3.6. The performance of each MSJC wall type is noted throughout the section. Twenty-nine of the sixty-seven walls examined in the study were classified as failing in flexure. Of the twenty-nine flexural failures, seventeen met MSJC provisions for special, nine met provisions for intermediate, and three met provisions for ordinary. Three ordinary walls met the prescriptive reinforcement requirements but were so heavily reinforced that they were downgraded in accordance with the provisions of Section 3.3.3.5 of the MSJC.

4.2.1 Performance With Respect to Ductility and Drift

MSJC wall classifications are established with the intent that different ductility levels are achieved with different wall types. Special walls are expected to provide the highest level of ductility and ordinary walls the lowest level. Drift values are subject to the same assumption for each wall classification. The highest drift values should be achieved in special walls and the lowest in ordinary walls. Ideally the ductility and drift values of walls belonging to the same MSJC wall classification would be similar, and these values would increase as you moved from ordinary to intermediate and from intermediate to special. The ratio of experimental moment capacity to nominal moment capacity should be near one in all cases where flexural failure is dominant. Evaluation of the data investigates these assumptions. Table 4.1 lists the mean, standard deviation (SD), and coefficient of variation (COV) for ductility, drift, and strength ratios according to the MSJC wall type. Figure 4.1 plots the ductility and drift values against the strength ratio.

The mean values of ductility are as anticipated as the special walls exhibit the highest ductility followed by intermediate and ordinary walls. The large standard deviation and COV values for ductility and drift demonstrate the significant scatter in the data for all wall types. This is also seen in Figure 4.1 where for special walls there is a significant difference between the maximum and minimum ductility values (12.2 – 3.06). The classification criteria of the walls accounts for some of the scatter. The flexural data set contains not only pure flexural failures but also several mixed forms of failure including flexure/shear modes. Walls failing in shear would be expected to exhibit lower levels of ductility. Significant shear deformations during testing would lead to failure prior to the wall reaching its full flexural capacity, and thus reduced ductility.

On average, the special walls exceeded their anticipated moment capacity while intermediate and ordinary walls fell just short of anticipated capacity. All walls were expected to reach or slightly exceed the expected moment capacity if the flexural failure mode was dominant. Four of the seven intermediate walls failed due to a mixed flexure/shear mechanism; thus, it is not surprising that on average they were below the anticipated moment capacity and below the values achieved by the ordinary walls. All three of the ordinary walls were reported to be flexural failures without any significant contributions from shear.

All of the wall types achieved an average drift of 1% or larger. Only four of the twenty-nine flexural walls looked at in the study fell short of 1% drift. All of the special walls surpassed a drift of 1.25%. The intermediate walls were surpassed in performance by the ordinary walls with respect to drift, but this can again be attributed to shear distress influencing the failure mode in these walls.

Table 4.1 Statistical results for ductility, drift, and strength ratios for walls failing in flexure

		Special	Int.	Ord.
Mean	Ductility	7.00	6.25	2.69
	Drift (%)	1.75	1.24	1.49
	M_{exp}/M_n	1.07	0.94	0.99
Standard Deviation	Ductility	2.80	3.20	0.50
	Drift (%)	0.43	0.60	0.18
	M_{exp}/M_n	0.09	0.14	0.11
Coefficient of Variation	Ductility	0.40	0.51	0.19
	Drift (%)	0.25	0.48	0.12
	M_{exp}/M_n	0.08	0.15	0.11
Number of Walls		17	9	3

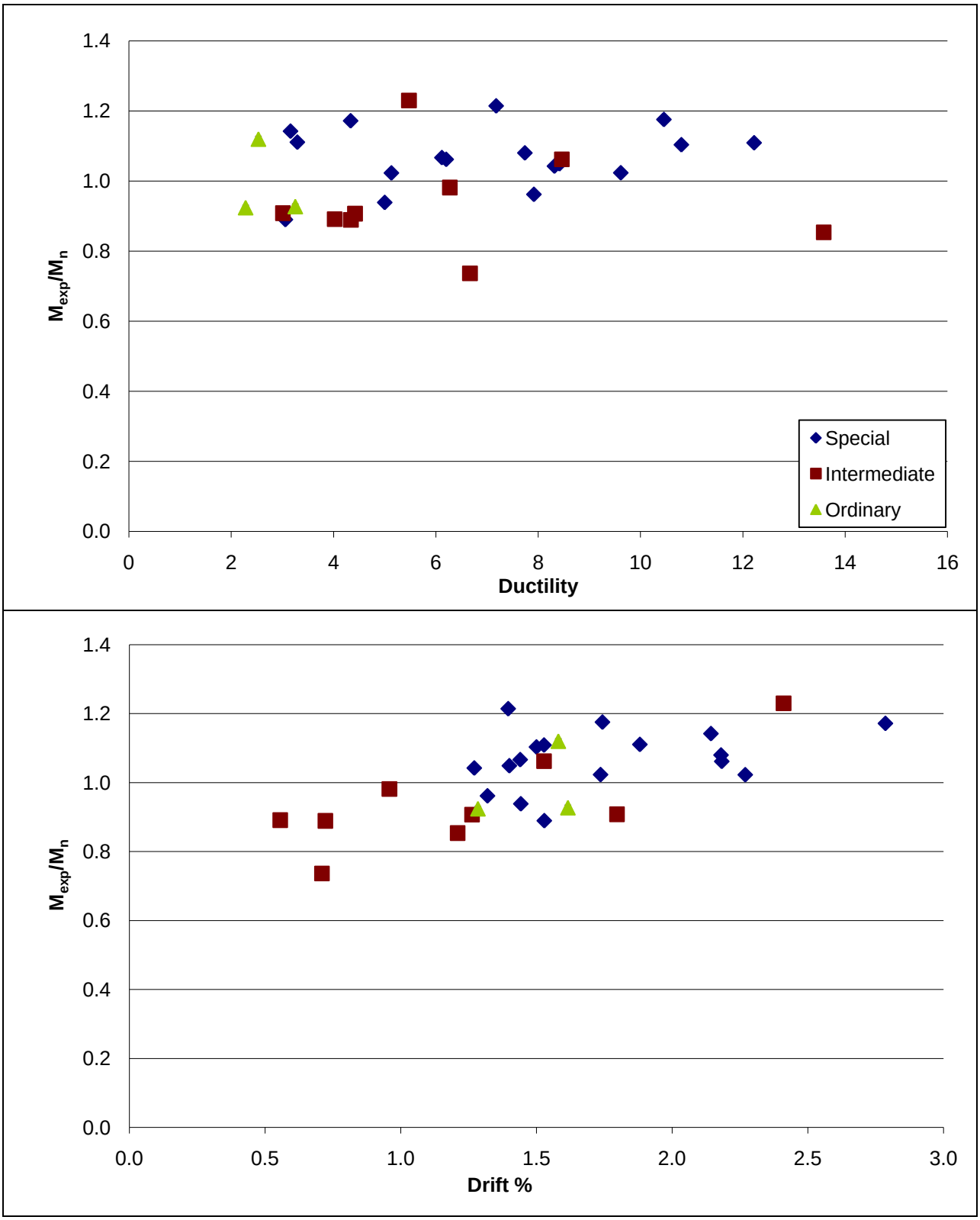

Figure 4.1 Ductility and drift in comparison to flexural strength ratio

4.2.2 Performance With Respect to Theoretical Predictions

Theoretical values of yield displacement, ultimate displacement, and displacement ductility were calculated for all twenty-nine walls failing in flexure. The ratio of the experimental value to the theoretical value for each parameter is presented in Table 4.2. The mean value, standard deviation, coefficient of variation, maximum, and minimum values are given.

Table 4.2 Ratios of experimental to theoretical values for ductility and displacements

	$\mu_\Delta/\mu_{\Delta,th}$	$\Delta_u/\Delta_{u,th}$	$\Delta_y/\Delta_{y,th}$
Mean	1.44	2.13	1.66
SD	0.56	0.68	0.77
COV	0.39	0.32	0.46
Max.	2.79	3.72	3.35
Min.	0.69	1.15	0.80

The mean ratio of experimental ductility to theoretical ductility is noticeably greater than one, indicating that on average the ductility observed during testing exceeded the ductility predicted from theoretical calculations. Ayers (2000) noted that the ultimate limit state used in his work was conservative, and thus it is reasonable that conservative values of ductility and ultimate displacement would be obtained. In the theoretical equations, the ultimate state is defined by a masonry compressive strain of 0.003 and 0.004 for concrete and clay masonry, respectively. In the calculation of experimental ductility, the ultimate state was defined at 20% strength degradation. It is likely that the strains at the experimental ultimate state were greater than those considered in the theoretical ultimate state. The experimental ultimate displacement was on average more than twice the theoretical ultimate displacement, demonstrating the conservative nature of the theoretical predictions.

Appreciable scatter in the data is shown by the standard deviation and the wide range between the maximum and minimum value. Some of the walls considered in the flexural data included mixed failure modes with significant shear and sliding responses. Ayers (2000) work was based on the assumption that the walls behaved in strictly a flexural manner. The existence of shear and sliding deformations increases the total wall displacements and contributed to the scatter in the data as well as to the conservative nature of the theoretical values.

4.2.3 Performance With Respect to Other Parameters

Performance of the walls was also evaluated by isolating the effects of individual parameters on the wall ductility and drift. The effect of individual specimen parameters on wall performance was evaluated through the use of data plots. Each parameter was isolated and plotted against ductility and drift values in order to look for trends and relationships between the parameter and ductility or drift. Trend lines and R^2 values were added (if sufficient data was available) in order to facilitate the recognition of the effect of the parameter on ductility or drift. An R^2 value near one indicates a strong correlation, while an R^2 value below 0.3 indicates a poor fit between the trend line and data. The following discussion compares the expected effect of the parameter (from theory or from prior studies) to the effect observed in this study.

4.2.3.1 Aspect Ratio

The ductility of walls observed in this study tended to decrease with an increase in aspect ratio, as seen in Figure 4.2. This is in accordance with theoretical predictions made by Paulay and Priestley (1992) that were presented in Section 2.3.2 in the form of Equation 2-3. Also notable is the effect of aspect ratio on drift. Taller, more slender walls exhibited higher drift

levels than shorter, squat walls. This can likely be attributed to the reduced stiffness of slender walls. However, the R^2 values indicate that the correlation is not strong for either trend.

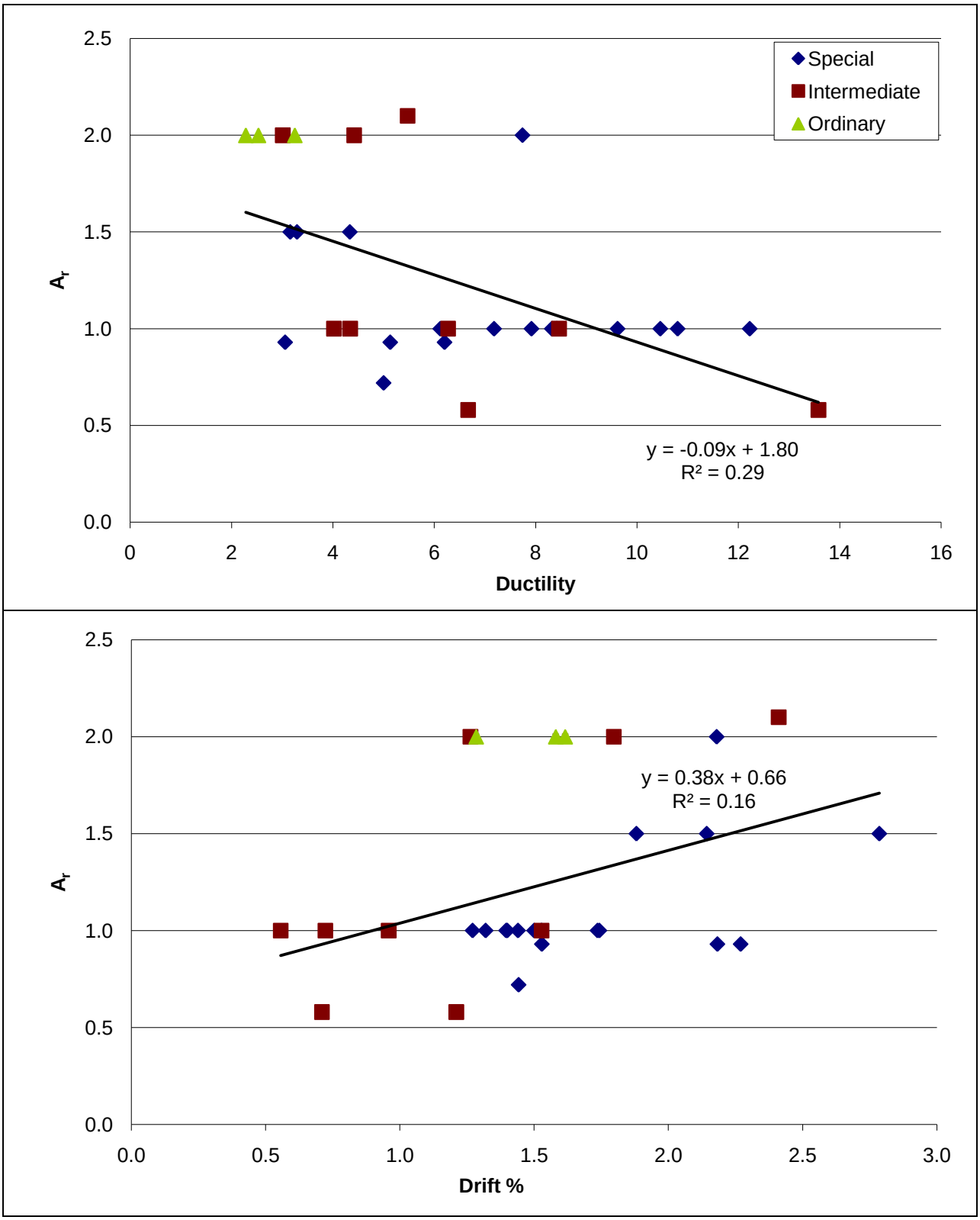

Figure 4.2 Ductility and drift in comparison to aspect ratio for walls failing in flexure

4.2.3.2 Horizontal Reinforcement Ratio

Higher levels of ductility are seen with increased amounts of horizontal reinforcement, as shown in Figure 4.3. The trend is as expected as higher levels of horizontal reinforcement protect against brittle shear failures and ensure that flexural failure and plastic hinging occurs. Shing et al. (1990) noted that increasing the horizontal reinforcement can significantly improve ductility in a wall dominated by shear, and the findings in this study agree with this assessment. Sveinsson et al. (1985) reported a positive correlation between increased horizontal reinforcement and improved inelastic behavior although the improvement was not proportional to the increase in reinforcement. Figure 4.3 is in agreement with that assessment. The level of horizontal reinforcement appears to have no effect on the drift capacity of a masonry shear wall failing in flexure. There is significant scatter among the data and almost no correlation with the linear trend line as indicated by the R^2 value. This indicates that the horizontal reinforcement does not affect the drift capacity for a wall failing in flexure.

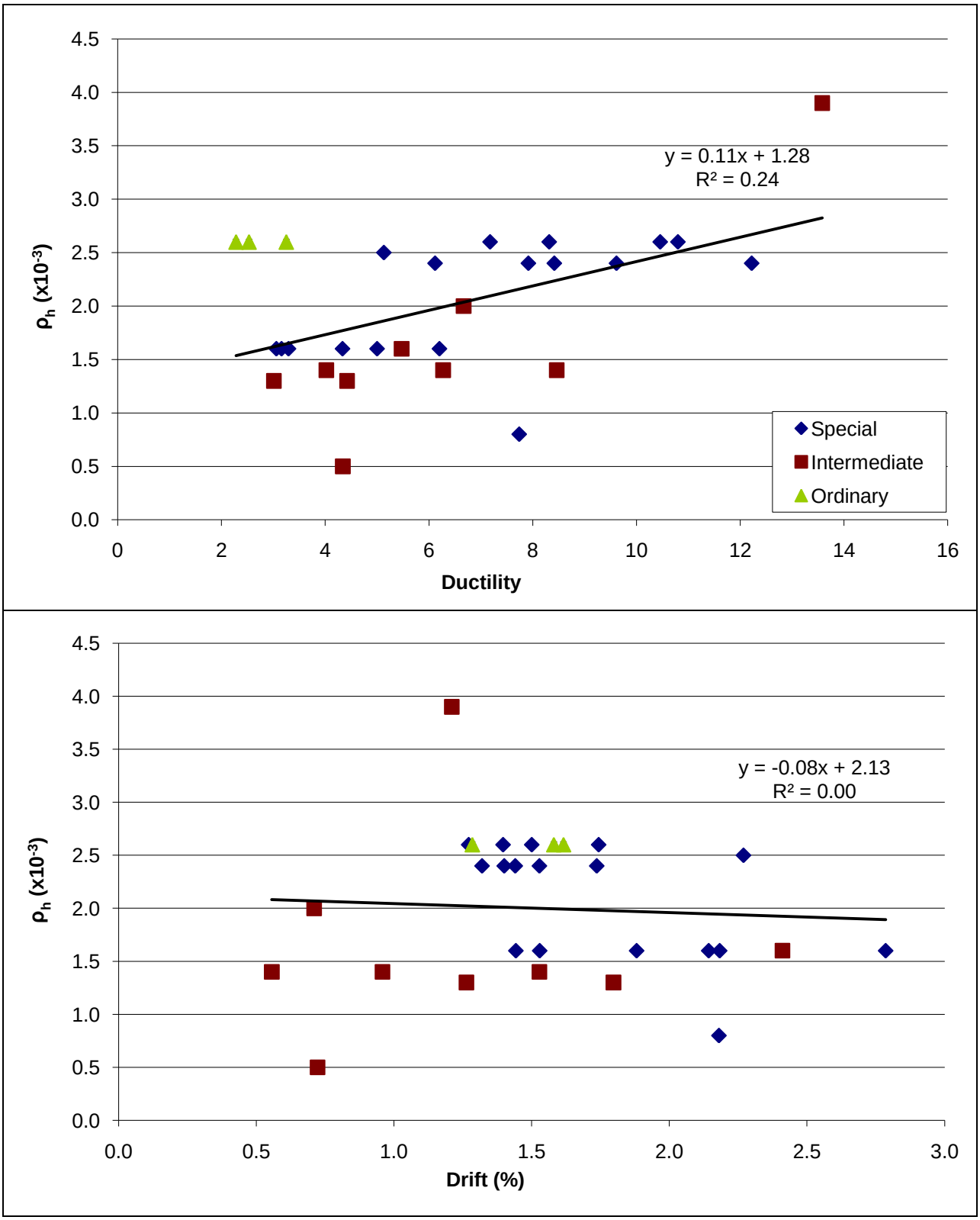

Figure 4.3 Ductility and drift in comparison to horizontal reinforcement ratio for walls failing in flexure

4.2.3.3 Vertical Reinforcement Ratio

The vertical reinforcement ratio is plotted against ductility and drift in Figure 4.4. A notable decrease in ductility is seen with increased levels of vertical reinforcement. This trend is in agreement with findings by other researchers and is consistent with the intent of the provisions in the MSJC. Paulay and Priestley (1992) and Shedid (2008) both reported reduced ductility due to higher levels of vertical reinforcement on the basis of theoretical and experimental findings. Provisions in the MSJC specifically limit the amount of flexural reinforcement (as discussed in Section 2.5) to ensure that adequate yielding of longitudinal reinforcement occurs prior to reaching critical compressive strains in the masonry. The effect on ductility seems to be most pronounced at very high levels of vertical reinforcement with a reduced effect as the level of reinforcement is diminished.

The data indicates that the level of vertical reinforcement has essentially no effect on the drift capacity of a wall failing in flexure. Noticeable scatter is evident in the plot and an R^2 of 0.01 is indicative of the poor fit between the linear trend line and the data.

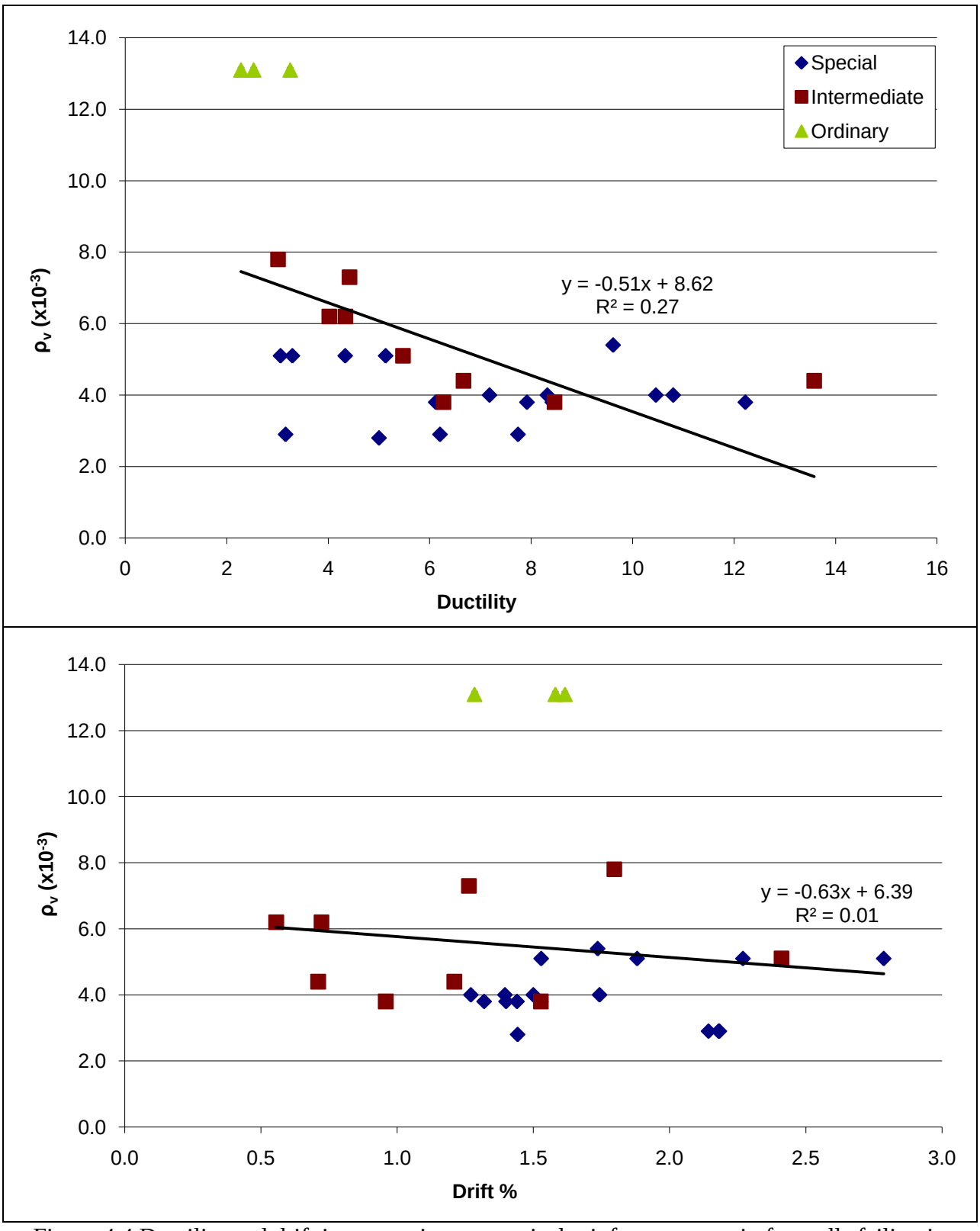

Figure 4.4 Ductility and drift in comparison to vertical reinforcement ratio for walls failing in flexure

4.2.3.4 Axial Compressive Stress

Findings from previous studies have indicated that increased levels of axial stress will result in reduced ductility in walls failing in flexure (Shing et al., 1990; Paulay and Priestley, 1992; Shedid, 2008). Early onset of toe crushing in the compressive region of the masonry in walls with high axial stress causes failure to occur at smaller displacements and thus reduces ductility. The findings in this study appear to be contradictory to previous findings as there is a trend toward increased ductility with increased compressive stress for walls failing due to flexure (as seen in Figure 4.5). One possible explanation is that the applied levels of compressive stress in this study were not large enough to significantly impact the crushing of masonry in critical regions.

Drift appears to be unaffected by the level of axial compression. The trend line indicates that walls with lower levels of axial compressive stress exhibit higher levels of drift. However the amount of scatter in the data and the poor fit between the trend line and the data indicate that no real trend can be taken from the plot. Once again this is likely due to the fact that the levels of applied axial compression are not large enough to significantly affect the wall performance.

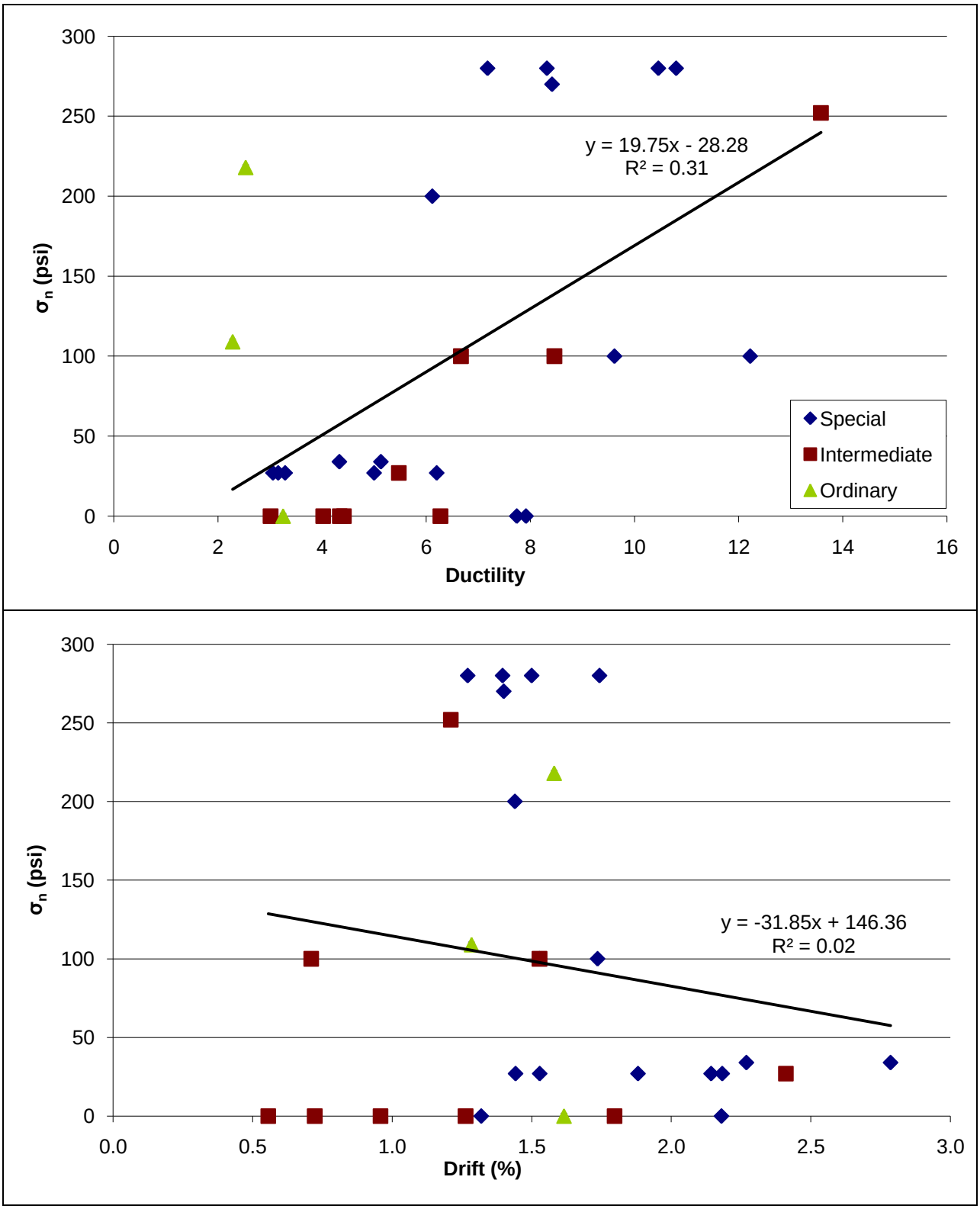

Figure 4.5 Ductility and drift in comparison to compressive stress for walls failing in flexure

4.3 Evaluation of Performance - Masonry Shear Walls Failing in Shear

The same analysis tools that were used for evaluating the performance of walls failing in flexure (Section 4.2) are now utilized in the following section to assess the performance of walls failing in shear. The performance of the walls is evaluated with respect to ductility and drift in Section 4.3.1. Performance with respect to other parameters is evaluated in Section 4.3.2. Thirty-eight of the sixty-seven walls examined in the study were classified as failing in shear. While there are more walls failing in shear than failing in flexure, the walls failing in shear are not as representative of all the MSJC wall types. Of the thirty-eight shear failures, only three walls met MSJC provisions for special and only four met provisions for ordinary. The remaining thirty-one walls fell into intermediate classification. It should also be noted that displacement ductility could not be calculated for one of the thirty-eight shear failures as an inadequate force-displacement envelope only displayed the latter half of the test. The ultimate displacement was determined from the end of the test, but the yield displacement could not be verified.

4.3.1 Performance With Respect to Ductility and Drift

Results of the statistical evaluation of the thirty-eight walls failing in shear are given in Table 4.3 and in Figure 4.6. The mean ductility values for each wall type generally follow expected trends. Special walls exhibited the highest ductility on average and ordinary walls exhibited the lowest. However, the reduction in ductility is not as extreme for walls failing in shear in comparison to walls failing in flexure. The mean ductility is also lower for special and intermediate wall types in comparison to the ductility values obtained for walls failing in flexure. Considerable scatter in the calculated ductility values was evident (as shown in Figure 4.6 and by the standard deviation values), although the scatter was not as extreme as the scatter seen in the

flexural wall data. The minimum calculated displacement ductility was 1.33 and the maximum was 10.0, indicating that adequately designed and detailed walls that fail in shear can still perform sufficiently during a seismic event.

The average drift values for each wall type are considerably lower than the average drift values for walls failing in flexure. The mean drift values for all wall types failing in shear is below 1%, and in the cases of intermediate and ordinary wall types the average drift is considerably below 1%. Approximately half of the walls analyzed in the shear failure data were tested under fixed-fixed conditions which cut the effective height of the walls in half. The reduced effective height and induced double bending along with earlier failure due to shear may have attributed to the reduced drift. The average drift values do trend as expected with special walls having the highest drift and ordinary walls the lowest.

Table 4.3 Statistical evaluation of ductility, drift, and strength ratios for walls failing in shear

		Special	Int.	Ord.
Mean	Ductility	5.00	4.93	4.06
	Drift (%)	0.94	0.70	0.56
	V_{exp}/V_n	1.16	1.16	1.31
Standard Deviation	Ductility	1.42	1.69	1.26
	Drift (%)	0.28	0.29	0.27
	V_{exp}/V_n	0.04	0.16	0.25
Coefficient of Variation	Ductility	0.28	0.34	0.31
	Drift (%)	0.30	0.41	0.48
	V_{exp}/V_n	0.04	0.14	0.19
Number of Walls		3	31	4

The shear capacity observed in testing exceeded the predicted shear capacity in all but 5 of the walls examined, and the majority of values of V_{exp}/V_n are very near 1.0. This indicates the accuracy of the MSJC provisions in estimating shear capacity and the adequate performance of

the walls. There is also a slight trend towards increased shear strength ratio with increased ductility.

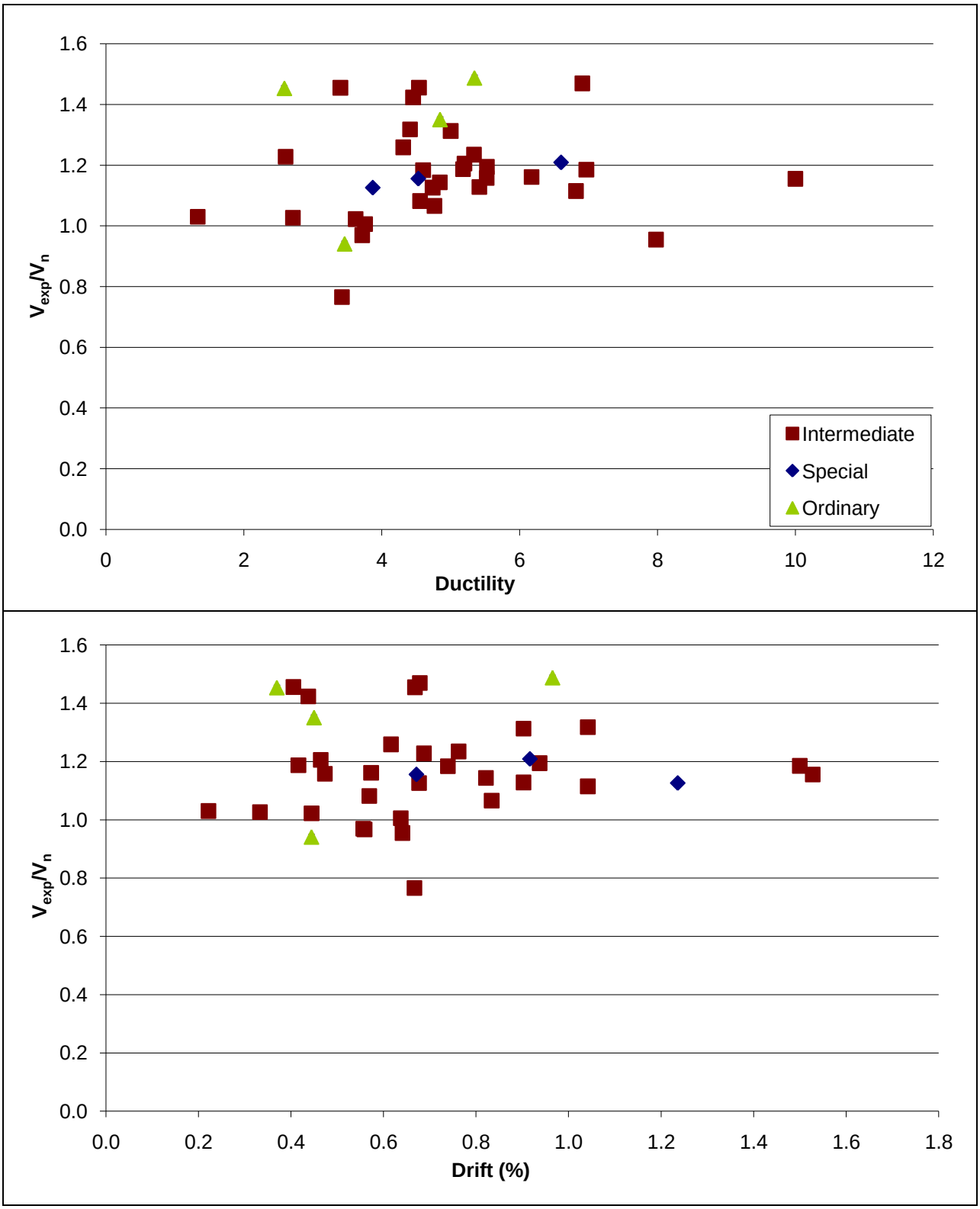

Figure 4.6 Ductility and drift in comparison to shear strength ratio for walls failing in shear

4.3.2 Performance With Respect to Other Parameters

Performance of walls failing in shear was also evaluated by isolating the effects of individual parameters on the wall ductility and drift. The subsequent sections present plots and discussion on the effects of aspect ratio (A_r), horizontal reinforcement ratio (ρ_h), vertical reinforcement ratio (ρ_v), and axial compressive stress (σ_n) on the performance of walls failing in shear.

4.3.2.1 Aspect Ratio

The relationship between aspect ratio, ductility, and drift is plotted in Figure 4.7. Displacement ductility decreased with increasing aspect ratio while drift increased with increasing aspect ratio. The reduction in ductility with increased aspect ratio is in agreement with theoretical and experimental findings from Paulay and Priestley (1992) as discussed in Section 4.2.3.1. Trends observed in Figure 4.7 are similar to the trends observed in Figure 4.2 for walls failing in flexure. The correlation is much weaker, however, and can be attributed to the lack of significant variation in aspect ratios in the experimental studies. Only three different aspect ratios were used in all of the experimental data for walls failing in shear, and only one test was conducted on a wall with an aspect ratio of 2.0. A wider range of aspect ratios would have likely revealed more satisfying conclusions about the effect of aspect ratio on ductility and drift. The extremely low R^2 values for both plots indicate that the trend lines are not indicative of the effect of aspect ratio on ductility or drift for walls failing in shear.

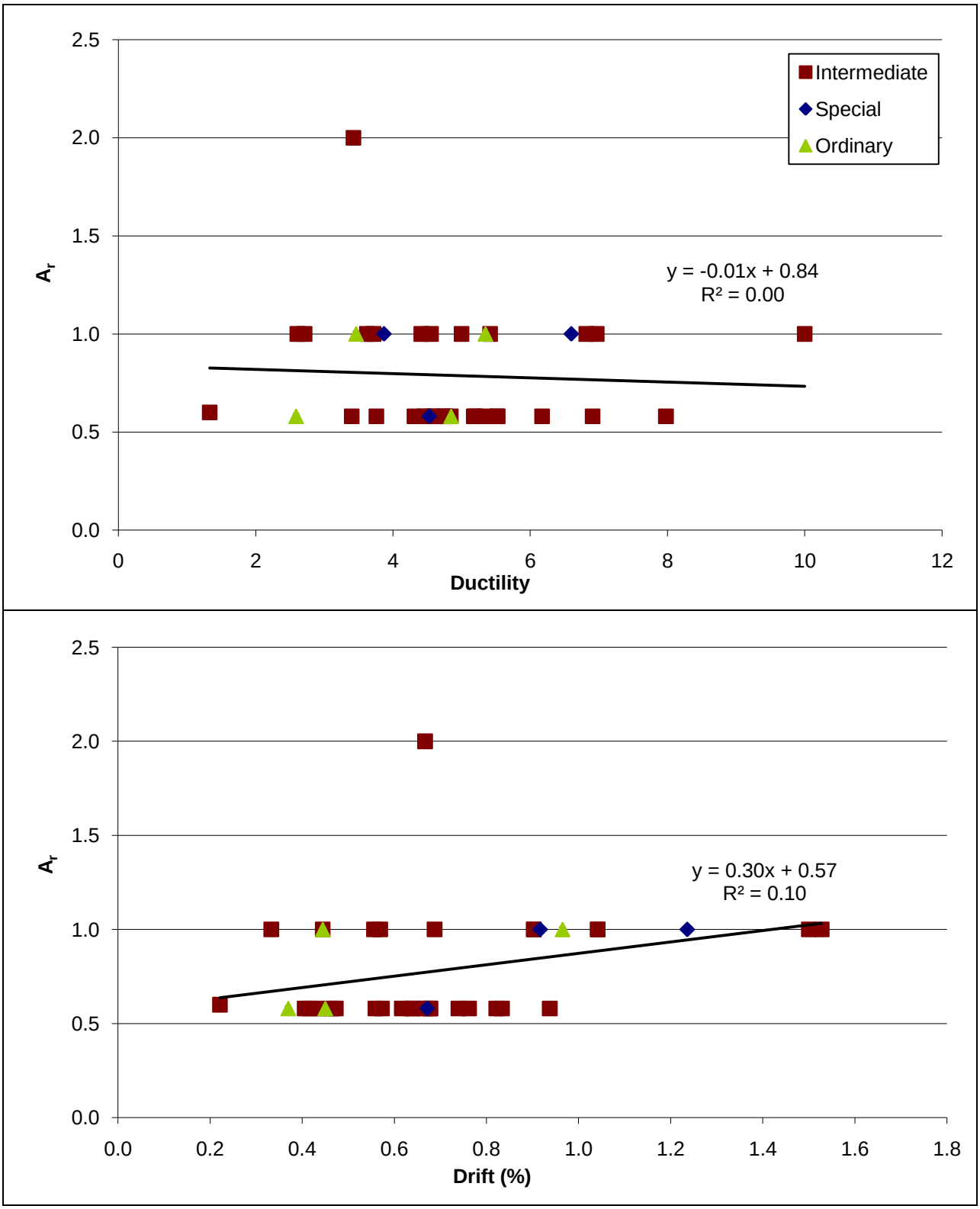

Figure 4.7 Ductility and drift in comparison to aspect ratio for walls failing in shear

4.3.2.2 Horizontal Reinforcement Ratio

Higher levels of ductility are seen with increased amounts of horizontal reinforcement, (as shown in Figure 4.8) although the fit between the trend line and the data is extremely poor. The poor fit of the trend line and the scatter in the data indicate that horizontal reinforcement does not affect ductility. This trend is not as expected for walls failing in shear. Increased levels of horizontal reinforcement protect against brittle shear failures as they enable the wall to sustain shear capacity even after diagonal cracking of the masonry has begun. Closely-spaced shear reinforcement has been shown to enable distribution of stresses along wall diagonals and limit the ability of existing cracks to widen. Instead new diagonal cracks form along the wall as lateral displacements increase, resulting in increased energy dissipation and improved ductile behavior (Voon and Ingham, 2006). Similar findings have been reported by Sveinsson et al. (1985) and Shing et al. (1990).

The effect on drift is expected to be similar to the effect on ductility. Walls failing in shear that are reinforced with higher levels of shear reinforcement should be able to withstand larger lateral displacements and thus should attain higher drift levels. The data assessed in this study generally agrees with this expectation, although again there is significant scatter in the data and almost no correlation between the trend line and the data itself (as seen in Figure 4.8).

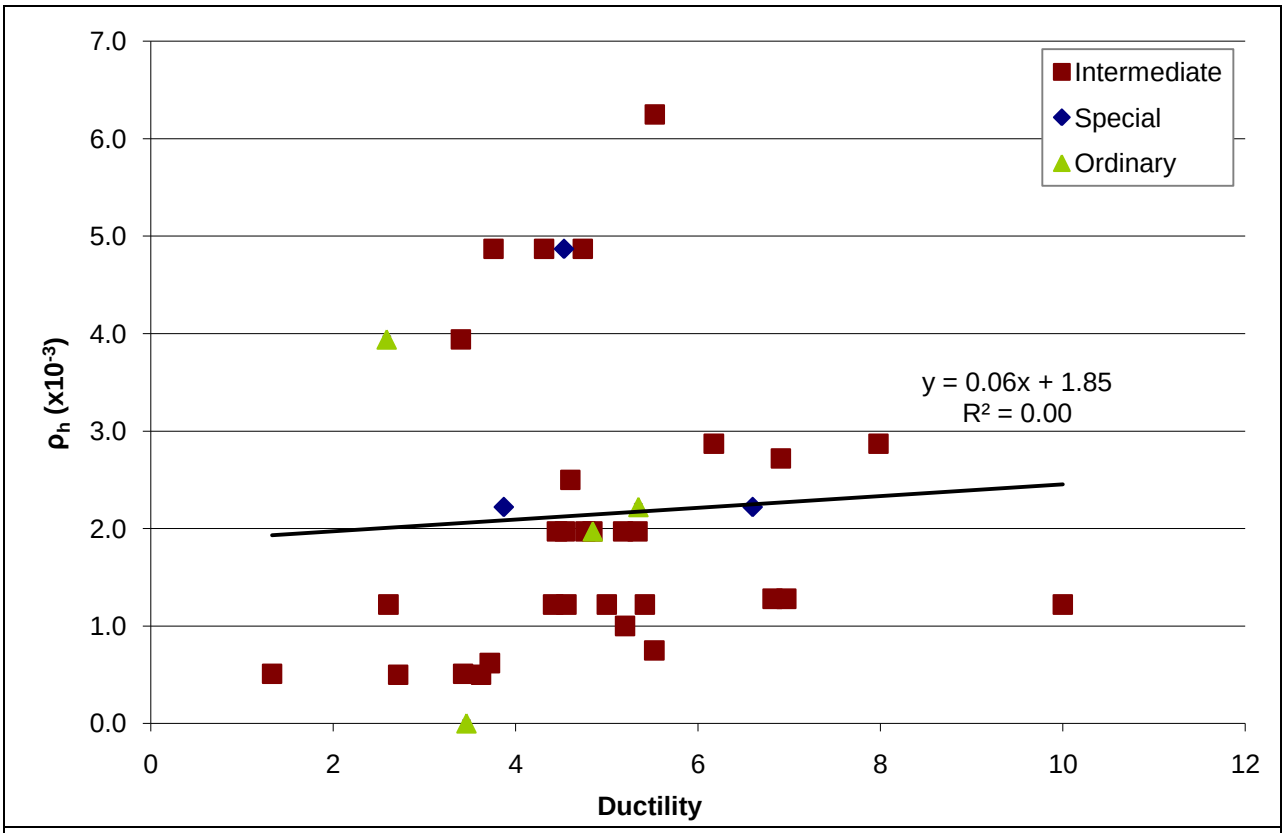

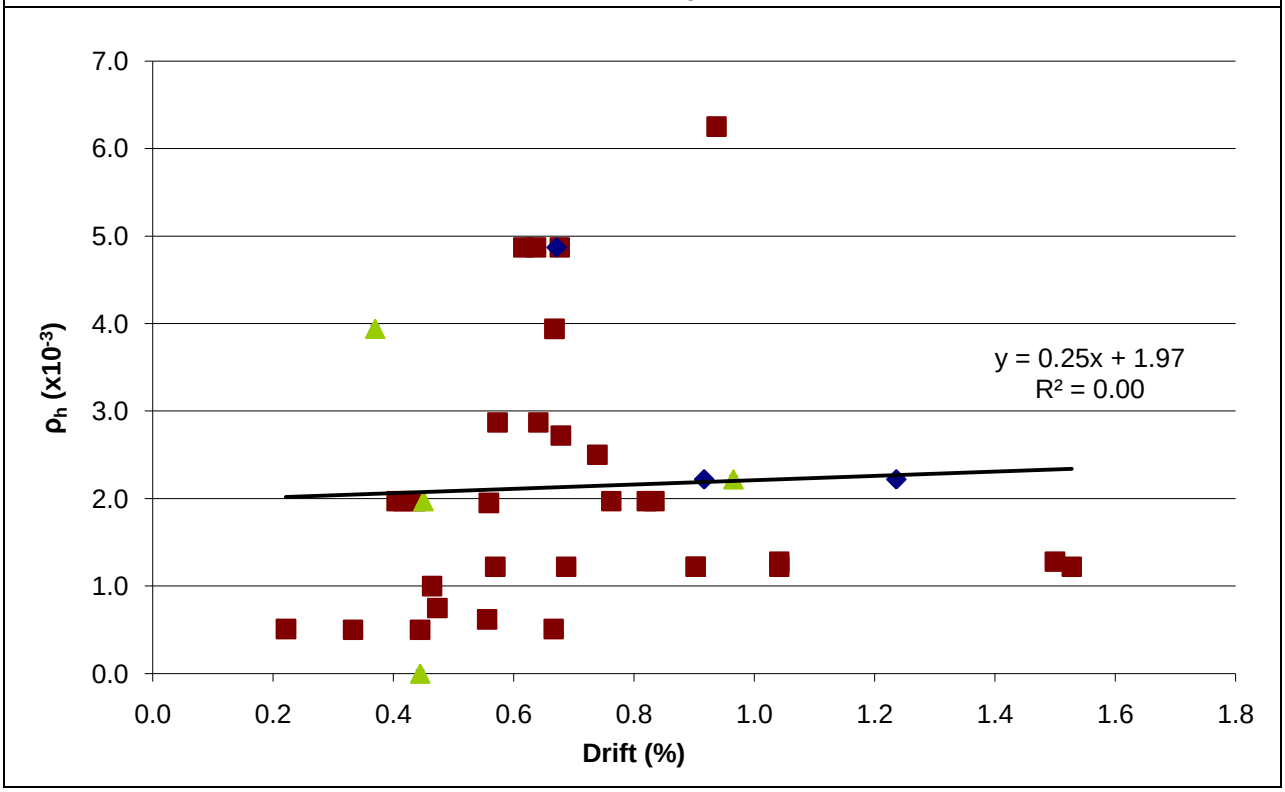

Figure 4.8 Ductility and drift in comparison to horizontal reinforcement ratio for walls failing in shear

4.3.2.3 Vertical Reinforcement Ratio

Increased levels of vertical reinforcement correlate with decreased levels of ductility, although the correlation is very weak (as seen in Figure 4.9). Other researchers have made similar conclusions based on theoretical and experimental studies as discussed in Section 4.2.3.3. The trend is not as strong as observed for walls failing in flexure (see Figure 4.4). One possible explanation is that adequate amounts of uniformly-distributed vertical reinforcement are needed to resist a shear sliding mechanism (Priestley, 1986). Increased amounts of vertical reinforcement enhance the clamping force between the wall and the base, which augments friction and effectively resists sliding. Thus, there is some benefit to ductility in terms of higher levels of vertical reinforcement for walls failing due to a shear/sliding mechanism.

There is significant scatter in the drift data, likely indicating that the vertical reinforcement ratio does not significantly impact drift capacity. Drift capacity is increased slightly by higher levels of vertical reinforcement (as indicated by the trend line) although the correlation is very weak. An increase in drift capacity with increased vertical reinforcement would likely be due to the elimination of sliding as discussed earlier.

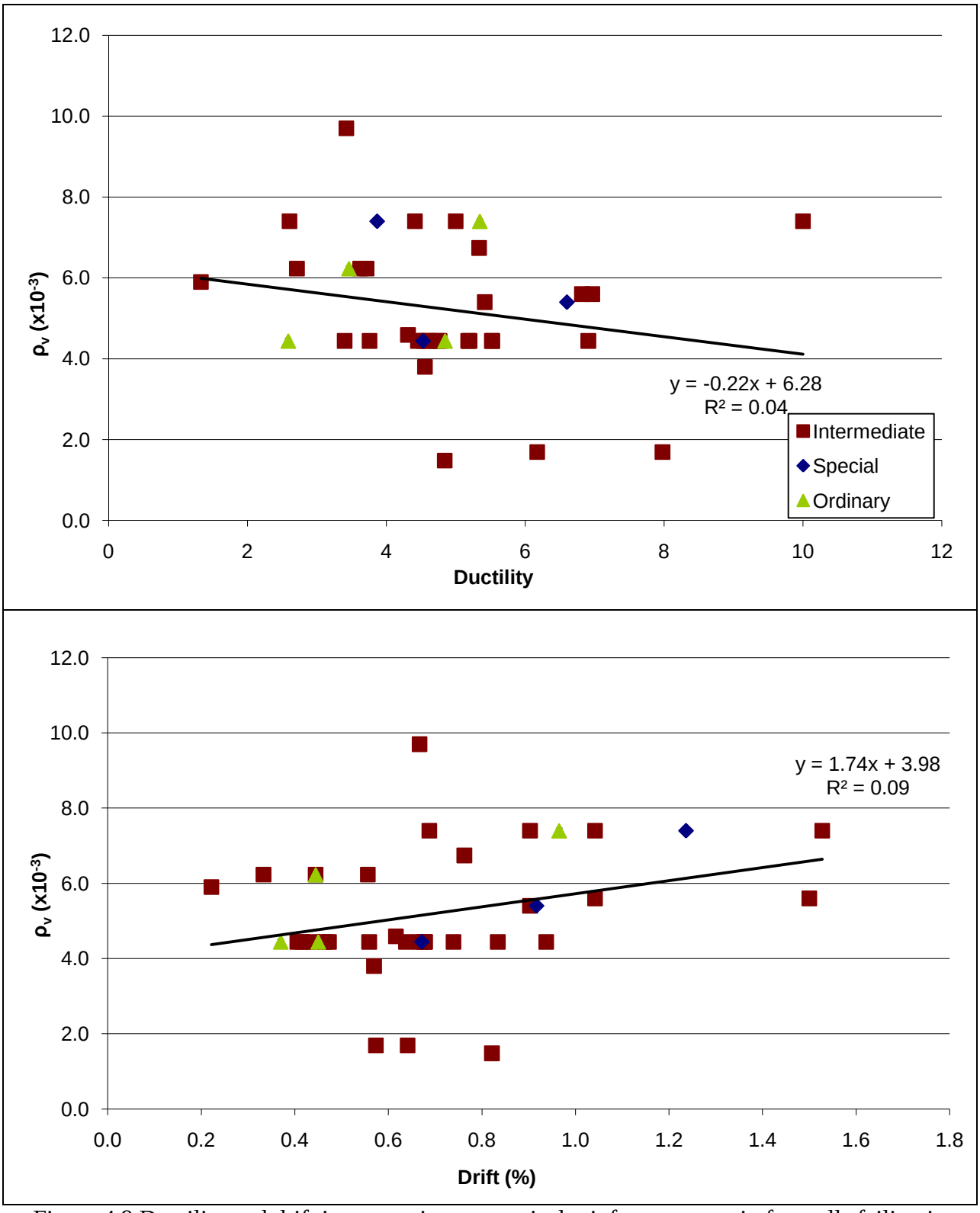

Figure 4.9 Ductility and drift in comparison to vertical reinforcement ratio for walls failing in shear

4.3.2.4 Axial Compressive Stress

Ductility and drift in shear-dominated walls are plotted against axial compressive stress in Figure 4.10. For shear-dominated walls, increased axial stress acts to offset tensile stresses in the masonry and delay the formation of diagonal tensile cracks caused by shear. This acts to increase the shear strength of the wall. However, the post-cracking deformation capacity of walls under increased axial load has been shown to decrease and the failure becomes more brittle. Previous studies have indicated that increased levels of axial stress will result in brittle failures and reduced ductility in walls failing in shear (Sveinsson et al., 1985; Shing et al., 1990; Paulay and Priestley, 1992). Similar to walls failing in flexure, the data for walls failing in shear trends in the opposite direction to expectations. Ductility actually increases with increased axial stress as seen in Figure 4.10. The correlation is very weak however, as indicated by the R^2 value of 0.10. It is more likely that there is no trend as the applied levels of axial load were not large enough to significantly impact post-cracking behavior and limit ductility.

Significant scatter exists in the drift data, but the general trend is toward decreased drift capacity with increased axial compression. As mentioned earlier, increased axial compression has been shown to make the failure mode more brittle and reduce drift capacity. Similar to the ductility data, the R^2 value is very low, indicating that low levels of axial compression do not affect drift capacity.

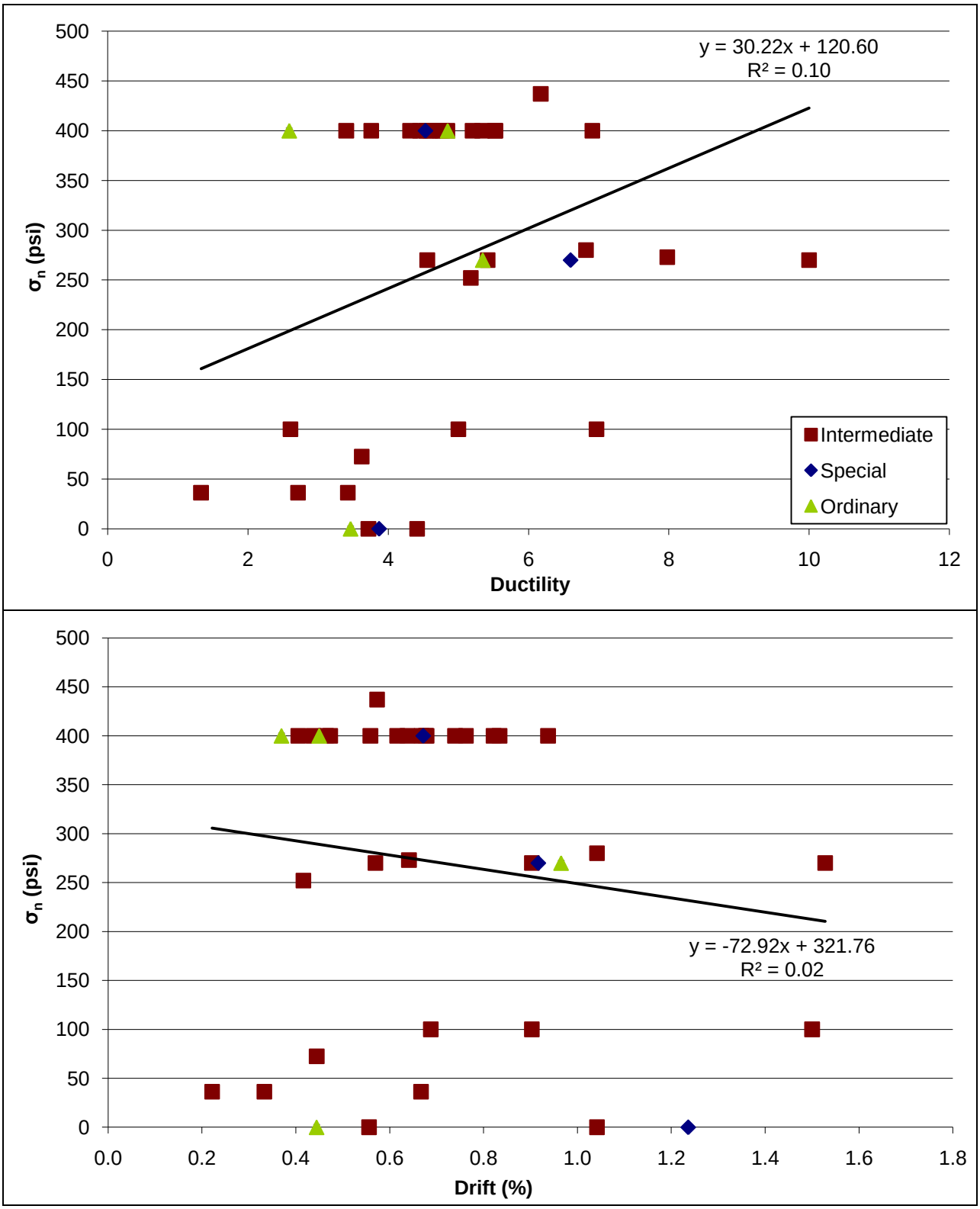

Figure 4.10 Ductility and drift in comparison to axial compressive stress for walls failing in shear

4.4 Summary – Performance of Masonry Shear Walls

Analysis of the experimental performance of the collected set of masonry shear wall tests yielded average values of ductility, drift, and strength ratios that in general were as anticipated. For both walls failing in flexure and failing in shear, the average ductility values trended as expected. Special walls exhibited the highest level of ductility, while ordinary walls exhibited the lowest. However, significant scatter was evident in both the flexural and shear ductility values, revealing a lack of consistency in producing a target level of ductility. The theoretical predictions for ductility capacity of walls failing flexure were largely conservative in comparison to the experimental values.

Average drift values followed similar trends to ductility values, with the exception that ordinary walls failing in flexure displayed a higher level of drift than intermediate walls failing in flexure. Substantial scatter was also observed in the drift data, but not to the extent seen in the ductility values. Notably, the average drift value of walls failing in flexure was above 1%, while walls failing in shear exhibited average values of drift below 1%. The reduced drift capacity of walls failing in shear is an indication of the brittle behavior that is generally associated with shear failures.

Analysis of the effect of individual parameters on ductility and drift in masonry shear walls generally followed expected trends observed in previous studies. Decreased levels of ductility and higher levels of drift were seen with higher aspect ratios. Ductility increased with increased levels of shear reinforcement. Increased vertical reinforcement resulted in decreased ductility, while there was no apparent effect on drift. The only significant trend observed that did not agree with theoretical analysis of masonry shear walls and with prior experimental studies was the trend toward increased ductility with increased axial compression. Drift capacity

was reduced however with increased axial compression. Many of the test parameter plots indicated that there was no apparent effect on ductility or drift. Significant scatter was observed and imposed linear trend lines had little to no correlation with the data. This indicated that for the given data there was no impact on ductility or drift for the given parameter.

CHAPTER 5

SUMMARY, CONCLUSIONS AND RECOMMENDATIONS

5.1 Summary

The research presented in this thesis investigated the structural performance of reinforced masonry shear walls conforming to requirements given in the 2008 MSJC *Building Code Requirements for Masonry Structures* under cyclic lateral loading. Seismic design provisions in the 2008 MSJC provide prescriptive requirements for three different wall types corresponding to different levels of expected performance and minimum levels of ductility during a seismic event. Ductility and drift values were obtained from a wide range of tests of masonry walls under simulated seismic loading. The test data consisted of results obtained for both fully grouted concrete and clay masonry walls. Each wall was classified to the applicable MSJC wall type and failure mode, and statistical analyses were performed to evaluate the performance of each wall type. Theoretical predictions of performance were compared to experimental results for walls failing in flexure. Parametric studies were also performed to evaluate the effects of various test parameters on ductility and drift.

Compilation of the data and subsequent statistical evaluation of ductility, drift, and strength ratios yielded the mean value for each MSJC wall type. An indication of the scatter in the data and subsequent reliability of the mean value provided by each wall type was determined through calculation of the standard deviation and coefficient of variation. The performance by each MSJC wall type was considered in comparison to anticipated performance. In addition, theoretical values of ductility and displacement were compared to experimental values for walls failing in flexure. The effects of individual parameters on ductility and drift were also

considered. Variables examined in the test specimens included different aspect ratios, reinforcement ratios, and levels of axial compressive stress. Conclusions and recommendations were then made based on the consistency of the performance of each wall type, the performance of the theoretical predictions of ductility and displacement, and the significant trends observed in the parameter analysis.

5.2 Conclusions

Results from this study indicate that the prescriptive provisions of MSJC Section 1.17 and limits on vertical reinforcement from Section 3.3.3.5 result in varying levels of ductility and performance for each wall type, as intended by the MSJC provisions. Special reinforced masonry walls exhibited higher levels of ductility on average than did intermediate walls, and intermediate walls surpassed ordinary walls. However, significant scatter in the data reveals that a specific level of ductility or performance in a wall type is difficult to achieve by meeting the prescriptive provisions alone. It is likely that wall performance was affected by other response modes, such as shear and sliding, which caused some variability in the results. Expanded research with walls failing only in flexure is recommended to further identify specific levels of ductility for each MSJC wall type.

The MSJC provisions result in an average drift capacity exceeding 1.2% for all wall types failing in flexure, while the average drift capacity for all wall types failing in shear was below 0.95% (considerably lower for intermediate and ordinary walls). These results indicate that for walls in which a ductile response is required, proper detailing must be provided (in addition to meeting prescriptive requirements) to ensure that shear failure does not occur. Failure should be controlled by flexural mechanisms, with damage occurring in properly detailed plastic hinges.

Evaluation of the effects of various parameters on shear wall performance largely aligned with results identified in previous research. Walls with small aspect ratios exhibited increased ductility capacity in comparison to walls with greater aspect ratios. Increased levels of horizontal reinforcement resulted in elevated levels of ductility, while larger vertical reinforcement ratios yielded lower levels of ductility. There was no statistical effect on ductility or drift for many of the wall parameters.

Results from the comparisons of theoretical ultimate displacements to experimental ultimate displacements in flexure-dominated walls indicate that the assumption that the ultimate limit state is controlled by compressive masonry strains of 0.003 or 0.004 is conservative in comparison to an ultimate limit state at 20% strength degradation. On average, the experimental ultimate displacement was more than twice as large as the theoretical ultimate displacement. Values of ultimate masonry compressive strain larger than 0.003 (unconfined concrete) and 0.004 (unconfined clay) should be considered when making theoretical predictions on the performance and ductility of masonry walls at 20% strength degradation. Additional research is recommended to identify strain values that correlate with a 20% loss in strength and that can then be used to calculate appropriate ultimate curvatures and more accurate ultimate displacements.

REFERENCES

Ayers, J.P., (2000) "Evaluation of Parameters for Limit States Design of Masonry Walls." MS Thesis, North Carolina State University, Raleigh, USA, 100pp

Davis, C.L., (2008) "Evaluation of Design Provisions for In-Plane Shear in Masonry Walls." M.S. Thesis, Department of Civil and Environmental Engineering, Washington State University, Pullman, WA.

Eikanas, I.K., (2003). "Behavior of Concrete Masonry Shear Walls with Varying Aspect Ratio and Flexural Reinforcement." M.S. Thesis, Department of Civil and Environmental Engineering, Washington State University, Pullman, WA.

National Earthquake Hazards Reduction Program (U.S.), NEHRP Recommended Provisions for Seismic Regulations for New Buildings and Other Structures - Part 2: Commentary. Washington, D.C.: Federal Emergency Management Agency, 2000.

NZS 4230:1990, "Code of Practice for the Design of Masonry Structures", Standards Association of New Zealand, Wellington.

Paulay, T. and Priestley M.J.N. (1992) Seismic Design of Reinforced Concrete and Masonry Buildings. New York: Wiley-Interscience.

Priestley, M.J.N. (1986). "Seismic Design of Concrete Masonry Shear Walls." ACI Journal, Vol. 83, No. 8, pp 58-68.

Priestley, M.J.N., Calvi, G., and Kowalsky, M., (2007). Displacement Based Seismic Design of Structures. (1st ed.). Pavia, Italy: IUSS Press.

Priestley, M.J.N. and Kowalsky, M.J., (1998). "Aspects of Drift and Ductility Capacity of Rectangular Cantilever Structural Walls," Bulletin NZNSEE, Vol. 31 (2), pp 73-85

Shedid, M.T. (2006). "Ductility of Reinforced Concrete Masonry Shear Walls." MASc thesis, Dept. of Civil Engineering, McMaster Univ., Hamilton, Ont., Canada.

Shedid, M.T., Drysdale, R.G., and El-Dakhakhni, W.W. (2008). "Behavior of Fully Grouted Reinforced Concrete Masonry Shear Walls Failing in Flexure: Experimental Results," Journal of Structural Engineering, Vol. 134, No. 11, 1754-1767.

Shing, P. B., Noland, J. L., Spaech, H., Klamerus, E., and Schuller, M. (1991), "Response of Single-Storey Reinforced Masonry Shear Walls to In-Plane Lateral Loads," TCCMAR Report 3.1(a)-2.

Shing, P. B., Schuller, M., and Hoskere, V. S. (1990), "In-Plane Resistance of Reinforced Masonry Shear Walls," ASCE Journal of Structural Engineering, Vol. 116, No. 3, pp. 619-640.

Snook, M.K., (2005). "Effects of Confinement Reinforcement on the Performance of Masonry Shear Walls." M.S Thesis, Department of Civil and Environmental Engineering, Washington State University, Pullman, WA.

Sveinsson, B. I., Mayes, R. L., and McNiven, H. D. (1985), "Cyclic Loading of Masonry Single Piers," Volume 4, Report No. UCB/EERC-85/15, Earthquake Engineering Research Centre, University of California, Berkeley.

TMS 402-08/ACI 530-08/ASCE 6-08. (2008), "Building Code Requirements and Specification for Masonry Structures," Masonry Standards Joint Committee.

Voon, K. C. (2007). "In-Plane Seismic Design of Concrete Masonry Structures." Thesis (PhD-Civil and Environmental Engineering)-University of Auckland.

Voon, K. C. and Ingham, J. M. (2006). "Experimental In-Plane Shear Strength Investigation of Reinforced Concrete Masonry Walls," Journal of Structural Engineering, Vol. 132, No. 3, 393-402.

Voon, K. C. and Ingham, J. M. (2007). "Design Expression for the In-Plane Shear Strength of Reinforced Concrete Masonry," Journal of Structural Engineering., Vol. 133, No. 5, 706-713.

XTRACT (Imbsen Software Systems 2005) Version 3.0.8, Imbsen & Associated Inc. Engineering Consultants. www.imbsen.com

APPENDIX A

WALL TEST DATA AND CALCULATIONS

Table A-1: Wall Test Data – Flexural Failure

Number	Label	Type	Failure	L_w (in.)	h_w (in.)	h_e (in.)	t (in.)	f'_m (psi)	f_{yv} (ksi)	ρ_v ($x10^{-3}$)
1	Shing - 1	S	F	72.0	72.0	72.0	5.63	2900	64.0	3.8
2	Shing - 2	S	F	72.0	72.0	72.0	5.63	2900	64.0	3.8
3	Shing - 6	I	F/S/SL	72.0	72.0	72.0	5.63	2600	64.0	3.8
4	Shing - 8	S	F/SL	72.0	72.0	72.0	5.63	3000	64.0	3.8
5	Shing - 10	I	F/S	72.0	72.0	72.0	5.63	3200	64.0	3.8
6	Shing - 12	S	F	72.0	72.0	72.0	5.63	3200	64.0	3.8
7	Shing - 15	S	F/S	72.0	72.0	72.0	5.63	3300	65.0	5.4
8	Shing - 17	S	F	72.0	72.0	72.0	5.38	3800	64.0	4.0
9	Shing - 18	S	F	72.0	72.0	72.0	5.38	3800	64.0	4.0
10	Shing - 19	S	F	72.0	72.0	72.0	5.38	3800	64.0	4.0
11	Shing - 20	S	F	72.0	72.0	72.0	5.38	3800	64.0	4.0
12	Snook - 1	S	F/S	55.6	52.0	52.0	7.63	1730	63.3	5.1
13	Snook - 2	S	F	55.6	84.0	84.0	7.63	1730	63.3	5.1
14	Shedid - 1	S	F	70.9	141.7	141.7	7.48	2470	72.8	2.9
15	Shedid - 2	I	F	70.9	141.7	141.7	7.48	2470	72.8	7.8
16	Shedid - 3	I	F	70.9	141.7	141.7	7.48	2470	72.8	7.3
17	Shedid - 4	O	F	70.9	141.7	141.7	7.48	2470	72.8	13.1
18	Shedid - 5	O	F	70.9	141.7	141.7	7.48	2470	72.8	13.1
19	Shedid - 6	O	F	70.9	141.7	141.7	7.48	2470	90.5	13.1
20	Voon - 1	I	F/S	70.9	70.9	70.9	5.51	2553	46.1	6.2
21	Voon - 3	I	F/SL	70.9	70.9	70.9	5.51	2466	46.1	6.2
22	Eikanas - 1	S	F/SL	55.6	52.0	52.0	7.63	1630	66.1	2.9
23	Eikanas - 2	S	F	55.6	84.0	84.0	7.63	1630	66.1	2.9
24	Eikanas - 4	S	F/S	55.6	52.0	52.0	7.63	1630	66.1	5.1
25	Eikanas - 5	S	F	55.6	84.0	84.0	7.63	1630	66.1	5.1
26	Eikanas - 6	I	F	39.6	84.0	84.0	7.63	1630	66.1	5.1
27	Eikanas - 7	S	F/S	71.6	52.0	52.0	7.63	1630	66.1	2.8
28	Sveinsson-19	I	F	48.0	56.0	28.0	5.63	2196	56.7	4.4
29	Sveinsson-22	I	F	48.0	56.0	28.0	5.63	2196	56.7	4.4

*Specimens with gray shading were constructed with Clay Masonry Units
Type: S=Special, I=Intermediate, O=Ordinary
Failure: F=Flexure, S=Shear, SL=Sliding

Table A-2: Wall Test Data – Flexural Failure

Number	f_{yh} (ksi)	ρ_h ($x10^{-3}$)	V_{max} (kips)	M_{max} (in-kips)	σ_n (psi)	A_r	d_{bl} (in.)	$M_{pred.}$ (in-kips)	$M_{exp}/M_{pred.}$	Δ_y (in.)	Δ_u (in.)
1	67.0	2.4	82.5	5940	200	1.00	0.625	5569	1.07	0.17	1.04
2	56.0	2.4	90.5	6516	270	1.00	0.625	6212	1.05	0.12	1.01
3	56.0	1.4	49.5	3564	0	1.00	0.625	3631	0.98	0.11	0.69
4	67.0	2.4	48.5	3492	0	1.00	0.625	3631	0.96	0.12	0.95
5	56.0	1.4	68.0	4896	100	1.00	0.625	4610	1.06	0.13	1.10
6	67.0	2.4	71.0	5112	100	1.00	0.750	4610	1.11	0.09	1.10
7	67.0	2.4	88.0	6336	100	1.00	0.625	6192	1.02	0.13	1.25
8	67.0	2.6	99.5	7164	280	1.00	0.625	6493	1.10	0.10	1.08
9	67.0	2.6	94.0	6768	280	1.00	0.625	6493	1.04	0.11	0.92
10	67.0	2.6	106.0	7632	280	1.00	0.625	6493	1.18	0.12	1.26
11	67.0	2.6	109.5	7884	280	1.00	0.625	6493	1.21	0.14	1.01
12	65.2	2.5	67.9	3531	34	0.93	0.625	3452	1.02	0.23	1.18
13	65.2	1.6	48.2	4045	34	1.50	0.625	3452	1.17	0.54	2.34
14	71.0	0.8	29.8	4224	0	2.00	0.591	3910	1.08	0.40	3.09
15	71.0	1.3	57.4	8135	0	2.00	0.787	8957	0.91	0.85	2.55
16	71.0	1.3	53.1	7526	0	2.00	0.787	8297	0.91	0.41	1.79
17	71.0	2.6	83.2	11792	0	2.00	0.984	12720	0.93	0.71	2.29
18	71.0	2.6	88.1	12486	109	2.00	0.984	13515	0.92	0.80	1.82
19	71.0	2.6	123.5	17504	218	2.00	0.984	15630	1.12	0.89	2.24
20	47.1	0.5	47.2	3345	0	1.00	0.787	3762	0.89	0.12	0.51
21	46.4	1.4	47.0	3331	0	1.00	0.787	3737	0.89	0.10	0.39
22	64.1	1.6	48.7	2530	27	0.93	0.625	2383	1.06	0.18	1.14
23	64.1	1.6	32.4	2722	27	1.50	0.625	2383	1.14	0.57	1.80
24	64.1	1.6	59.2	3078	27	0.93	0.625	3460	0.89	0.26	0.80
25	64.1	1.6	45.8	3843	27	1.50	0.625	3460	1.11	0.48	1.58
26	64.1	1.6	25.5	2138	27	2.10	0.625	1738	1.23	0.37	2.03
27	64.1	1.6	69.8	3630	27	0.72	0.625	3867	0.94	0.15	0.75
28	63.5	3.9	89.0	2504	252	0.58	0.875	2933	0.85	0.05	0.68
29	63.5	2.0	61.3	1725	100	0.58	0.875	2342	0.74	0.06	0.40

Table A-3: Wall Test Data – Flexural Failure

Number	μ_Δ	Drift %	φ_y (1/in.) (x 10^{-5})	φ_u (1/in.) (x 10^{-4})	L_p (in.)	μ_φ	$\Delta_{y,th}$ (in.)	$\Delta_{u,th}$ (in.)	$\mu_{\Delta,th}$	$\mu_\Delta/\mu_{\Delta,th}$	$\Delta_u/\Delta_{u,th}$	$\Delta_y/\Delta_{y,th}$
1	6.12	1.44	6.44	4.03	17.6	6.26	0.111	0.488	4.38	1.396	2.133	1.528
2	8.42	1.40	6.44	4.03	17.6	6.26	0.111	0.488	4.38	1.920	2.072	1.079
3	6.27	0.96	6.44	4.03	17.6	6.26	0.111	0.488	4.38	1.431	1.415	0.989
4	7.92	1.32	6.44	4.03	17.6	6.26	0.111	0.488	4.38	1.806	1.949	1.079
5	8.46	1.53	6.44	4.03	17.6	6.26	0.111	0.488	4.38	1.930	2.256	1.169
6	12.22	1.53	6.44	4.03	17.6	6.26	0.111	0.488	4.38	2.788	2.256	0.809
7	9.62	1.74	6.54	4.03	17.6	6.16	0.113	0.488	4.32	2.227	2.562	1.151
8	10.80	1.50	6.44	5.12	17.6	7.95	0.111	0.608	5.47	1.976	1.777	0.899
9	8.32	1.27	6.44	5.12	17.6	7.95	0.111	0.608	5.47	1.522	1.505	0.989
10	10.46	1.74	6.44	5.12	17.6	7.95	0.111	0.608	5.47	1.914	2.065	1.079
11	7.18	1.40	6.44	5.12	17.6	7.95	0.111	0.608	5.47	1.314	1.653	1.259
12	5.13	2.27	8.24	5.22	13.4	6.33	0.074	0.341	4.59	1.117	3.459	3.095
13	4.33	2.79	8.24	5.22	14.8	6.33	0.194	0.693	3.57	1.213	3.379	2.785
14	7.74	2.18	7.44	4.10	20.4	5.51	0.498	1.399	2.81	2.757	2.209	0.801
15	3.01	1.80	7.44	4.09	20.4	5.50	0.498	1.396	2.80	1.074	1.824	1.698
16	4.42	1.26	7.44	4.09	20.4	5.50	0.498	1.396	2.80	1.577	1.282	0.813
17	3.25	1.62	7.44	4.08	22.2	5.48	0.498	1.466	2.94	1.104	1.562	1.415
18	2.28	1.28	7.44	4.08	22.2	5.48	0.498	1.466	2.94	0.775	1.242	1.602
19	2.53	1.58	9.25	4.08	27.0	4.41	0.619	1.712	2.77	0.915	1.308	1.429
20	4.34	0.72	4.71	4.09	11.2	8.69	0.079	0.343	4.35	0.997	1.493	1.496
21	4.02	0.56	4.71	4.09	11.2	8.69	0.079	0.343	4.35	0.924	1.149	1.243
22	6.20	2.18	8.61	5.22	13.4	6.07	0.078	0.342	4.42	1.405	3.314	2.359
23	3.16	2.14	8.61	5.22	14.8	6.07	0.202	0.697	3.45	0.916	2.581	2.816
24	3.06	1.53	8.61	5.22	13.4	6.06	0.078	0.342	4.41	0.693	2.323	3.352
25	3.29	1.88	8.61	5.22	14.8	6.06	0.202	0.697	3.44	0.956	2.267	2.372
26	5.47	2.41	1.21	7.32	13.0	6.06	0.284	0.900	3.17	1.729	2.251	1.302
27	5.00	1.44	6.68	4.05	16.6	6.07	0.060	0.306	5.08	0.984	2.450	2.490
28	13.58	1.21	8.55	6.05	15.0	7.07	0.022	0.182	8.16	1.665	3.724	2.237
29	6.67	0.71	8.55	6.05	15.0	7.07	0.022	0.182	8.16	0.817	2.194	2.684

Table A-4: Wall Test Data – Shear Failure

Number	Label	Type	Failure	L_w (in.)	h_w (in.)	h_e (in.)	t (in.)	f'_m (psi)	f_{yv} (ksi)	ρ_v ($x10^{-3}$)	σ_n (psi)
30	Sveinsson-13	I	S	48.0	56.0	28.0	7.63	3359	67.5	1.69	273
31	Sveinsson-15	I	S	48.0	56.0	28.0	7.63	3359	67.5	1.69	437
32	Sveinsson-17	I	S	48.0	56.0	28.0	5.63	2297	56.7	4.44	400
33	Sveinsson-18	O	S	48.0	56.0	28.0	5.63	2297	59.5	4.44	400
34	Sveinsson-20	I	S	48.0	56.0	28.0	5.63	2196	56.7	4.44	400
35	Sveinsson-21	O	S	48.0	56.0	28.0	5.63	2196	59.5	4.44	400
36	Sveinsson-23	I	S	48.0	56.0	28.0	5.63	2196	56.7	4.44	400
37	Sveinsson-24	I	S	48.0	56.0	28.0	5.63	2196	56.7	4.44	400
38	Sveinsson-25	I	S	48.0	56.0	28.0	5.63	2196	56.7	4.44	252
39	Sveinsson-26	I	S	48.0	56.0	28.0	5.63	2196	56.7	4.44	400
40	Sveinsson-19	I	S	48.0	56.0	28.0	5.63	2918	56.7	4.44	400
41	Sveinsson-20	I	S/SL	48.0	56.0	28.0	5.63	2918	56.7	4.44	400
42	Sveinsson-21	I	S	48.0	56.0	28.0	5.63	2918	56.7	6.74	400
43	Sveinsson-22	I	S/SL	48.0	56.0	28.0	5.63	2918	63.5	4.59	400
44	Sveinsson-23	I	S	48.0	56.0	28.0	5.63	2918	59.5	4.44	400
45	Sveinsson-24	S	S/SL	48.0	56.0	28.0	5.63	2918	59.5	4.44	400
46	Sveinsson-25	I	S	48.0	56.0	28.0	5.63	2918	56.7	1.48	400
47	Sveinsson-26	I	S/SL	48.0	56.0	28.0	5.63	2918	56.7	4.44	400
48	Sveinsson-27	I	S	48.0	56.0	28.0	5.63	2918	56.7	4.44	400
49	Sveinsson-28	I	S/SL	48.0	56.0	28.0	5.63	2918	59.5	4.44	400
50	Sveinsson-30	I	S	48.0	56.0	28.0	5.63	4008	56.7	4.44	400
51	Shing - 3	I	S	72.0	72.0	72.0	5.63	3000	72.0	7.40	270
52	Shing - 4	I	S	72.0	72.0	72.0	5.63	2600	72.0	7.40	0
53	Shing - 5	I	S	72.0	72.0	72.0	5.63	2600	72.0	7.40	100
54	Shing - 7	I	S	72.0	72.0	72.0	5.63	3000	72.0	7.40	100
55	Shing - 9	I	S	72.0	72.0	72.0	5.63	3000	64.0	3.80	270
56	Shing - 11	S	S/SL	72.0	72.0	72.0	5.63	3200	72.0	7.40	0
57	Shing - 13	S	S	72.0	72.0	72.0	5.63	3300	65.0	5.40	270
58	Shing - 14	I	S	72.0	72.0	72.0	5.63	3300	65.0	5.40	270
59	Shing - 16	O	S	72.0	72.0	72.0	5.63	2500	72.0	7.40	270
60	Shing - 21	I	S	72.0	72.0	72.0	5.38	3800	65.0	5.60	280
61	Shing - 22	I	S	72.0	72.0	72.0	5.38	3800	65.0	5.60	100
62	Voon - 2	O	S	70.9	70.9	70.9	5.51	2553	46.1	6.23	0
63	Voon - 4	I	S	70.9	70.9	70.9	5.51	2466	46.1	6.23	0
64	Voon - 7	I	S	70.9	70.9	70.9	5.51	2727	46.1	6.23	73
65	Voon - 8	I	S	70.9	70.9	70.9	5.51	2727	46.1	6.23	36
66	Voon - 9	I	S	70.9	141.7	141.7	5.51	3524	79.8	9.70	36
67	Voon - 10	I	S	118.1	70.9	70.9	5.51	3524	46.1	5.90	36

Table A-5: Wall Test Data – Shear Failure

Number	$f_{y\ hor.}$ (ksi)	ρ_h ($x10^{-3}$)	s_h (in.)	Ar	V_{max} (kips)	V_n (kips)	$V_{exp.}/V_n$	Drift %	Δ_y (in.)	Δ_u (in.)	μ_Δ
30	59.0	2.87	11.2	0.58	103.7	108.6	0.95	0.64	0.045	0.359	7.98
31	59.0	2.87	11.2	0.58	126.1	108.6	1.16	0.57	0.052	0.321	6.17
32	63.5	3.94	11.2	0.58	96.4	66.3	1.45	0.67	0.110	0.374	3.40
33	63.5	3.94	11.2	0.58	96.3	66.3	1.45	0.37	0.080	0.207	2.59
34	63.5	1.97	18.7	0.58	92.2	64.8	1.42	0.44	0.055	0.245	4.45
35	63.5	1.97	18.7	0.58	87.5	64.8	1.35	0.45	0.052	0.252	4.85
36	63.5	0.75	8.0	0.58	75.0	64.8	1.16	0.47	0.048	0.265	5.52
37	63.5	2.72	15.7	0.58	95.2	64.8	1.47	0.68	0.055	0.380	6.91
38	63.5	1.97	18.7	0.58	76.9	64.8	1.19	0.42	0.045	0.233	5.18
39	63.5	1.97	18.7	0.58	94.3	64.8	1.46	0.41	0.050	0.227	4.54
40	63.5	1.95	18.7	0.58	72.2	74.7	0.97	0.56	-	0.313	-
41	63.5	4.87	9.3	0.58	75.1	74.7	1.01	0.64	0.095	0.357	3.76
42	63.5	1.97	18.7	0.58	92.2	74.7	1.23	0.76	0.080	0.427	5.34
43	63.5	4.87	9.3	0.58	94.0	74.7	1.26	0.62	0.080	0.345	4.31
44	63.5	1.97	18.7	0.58	79.6	74.7	1.07	0.83	0.098	0.467	4.77
45	63.5	4.87	9.3	0.58	86.3	74.7	1.16	0.67	0.083	0.376	4.53
46	63.5	1.97	18.7	0.58	85.4	74.7	1.14	0.82	0.095	0.460	4.84
47	63.5	4.87	9.3	0.58	84.1	74.7	1.13	0.68	0.080	0.379	4.74
48	59.5	2.50	11.2	0.58	88.4	74.7	1.18	0.74	0.090	0.414	4.60
49	60.5	6.25	5.1	0.58	89.2	74.7	1.19	0.94	0.095	0.525	5.53
50	63.5	1.00	8.0	0.58	105.5	87.5	1.21	0.46	0.050	0.260	5.20
51	56.0	1.22	16.0	1.00	102.5	88.7	1.16	1.53	0.110	1.100	10.0
52	56.0	1.22	16.0	1.00	79.5	60.3	1.32	1.04	0.170	0.750	4.41
53	56.0	1.22	16.0	1.00	86.5	70.4	1.23	0.69	0.190	0.495	2.61
54	56.0	1.22	16.0	1.00	97.0	73.9	1.31	0.90	0.130	0.650	5.00
55	56.0	1.22	16.0	1.00	96.0	88.7	1.08	0.57	0.090	0.410	4.56
56	67.0	2.22	16.0	1.00	92.0	81.7	1.13	1.24	0.230	0.890	3.87
57	67.0	2.22	16.0	1.00	112.5	93.1	1.21	0.92	0.100	0.660	6.60
58	56.0	1.22	16.0	1.00	105.0	93.1	1.13	0.90	0.120	0.650	5.42
59	67.0	2.22	16.0	1.00	120.5	81.0	1.49	0.97	0.130	0.695	5.35
60	56.0	1.28	16.0	1.00	105.5	94.6	1.11	1.04	0.110	0.750	6.82
61	56.0	1.28	16.0	1.00	91.5	77.2	1.19	1.50	0.155	1.080	6.97
62	47.1	0.00	70.9	1.00	41.8	44.4	0.94	0.44	0.091	0.315	3.46
63	45.0	0.62	31.5	1.00	47.7	49.2	0.97	0.56	0.106	0.394	3.72
64	47.1	0.50	15.8	1.00	58.9	57.6	1.02	0.44	0.087	0.315	3.62
65	47.1	0.50	15.8	1.00	55.5	54.1	1.03	0.33	0.087	0.236	2.71
66	47.1	0.51	15.8	2.00	46.2	60.3	0.77	0.67	0.276	0.945	3.42
67	47.1	0.51	15.8	0.60	131.5	127.6	1.03	0.22	0.118	0.157	1.33